

# DISCRIMINATOR-GUIDED EMBODIED PLANNING FOR LLM AGENT

**Anonymous authors**

Paper under double-blind review

## ABSTRACT

Large Language Models (LLMs) have showcased remarkable reasoning capabilities in various domains, yet face challenges in complex embodied tasks due to coherent long-term policy, context-sensitive environmental understanding. Previous work performed LLM refinement relying on outcome-supervised feedback, which can be costly and ineffective. In this work, we introduce a novel framework, **Discriminator-Guided Action OPTimization (DGAP)** for facilitating optimization of LLM action plans via step-wise signals. Specifically, we employ a limited set of demonstrations to enable the discriminator in learning a score function, which assesses the alignment between LLM-generated action and the underlying optimal one at every step. Based on the discriminator, LLM is prompted to generate actions to maximize the score utilizing historical action-score pairs trajectory as guidance. Under mild conditions, DGAP resembles the critic-regularized optimization and is demonstrated to achieve a stronger policy than the LLM planner. In experiments across different LLMs (GPT-4, Llama3-70B) in ScienceWorld and VirtualHome, our method obtains superior performance and better efficiency than previous methods.

## 1 INTRODUCTION

The effectiveness of large language models (LLMs) in task planning hinges on their ability to generate coherent, executable plans in dynamic, open-ended environments (Song et al., 2023; Suzgun et al., 2022), in which embodied scenarios present greater challenges due to the need for long-term planning in more intricate contexts. Specifically, embodied planning presents challenge due to inherent complexities and error accumulation over extended horizons. It involves coordinating long action sequences while managing intricate, dynamic environments with high-dimensional state spaces and tangible interactions. Moreover, in long-term planning, initial inaccuracies compound over steps, causing significant deviations from the plan and risking mission failure (Ross et al., 2011; Luo et al., 2024).

Facing these difficulties, in-context learning methods (Dong et al., 2022; Abernethy et al., 2023; Akyürek et al., 2023), tree-of-thought(ToT) methods (Yao et al., 2023a; Feng et al., 2023; Zhou et al., 2023a) and demonstration-based methods (Lin et al., 2023; Rita et al., 2024) have accomplished partial progress. However, a key issue is that they generally receive feedback signals at the trajectory level, which is non-proactive and limits their effectiveness and generalization in dynamic embodied scenarios (Chen et al., 2024b; Liu et al., 2024; Shi et al., 2024). In particular, in-context learning methods introduce closed-loop feedback(Song et al., 2023; Wu et al., 2023) for failed results at completion via inner monologue (Madaan et al., 2023; Huang et al., 2022a; Yao et al., 2023b) or physical feedback (Shinn et al., 2023; Mandi et al., 2023). ToT methods (Yao et al., 2023a; Feng et al., 2023; Zhou et al., 2023a) generate multiple trajectories to represent several reasoning pathways, and perform trajectory-level switching optimization, which incurs high exploration costs (Zhang et al., 2024). Demonstration-based approaches require extensive, high-quality trajectories in diverse scenarios to obtain a generalized policy (Lin et al., 2023; Rita et al., 2024) (see Fig. 1).

In the light of these challenges, we consider an alternative way for grounding and generalization of embodied planning by leveraging the knowledge from limited demonstrations to construct step-level guidance, which is subsequently integrated into in-context learning to boost planning. A key

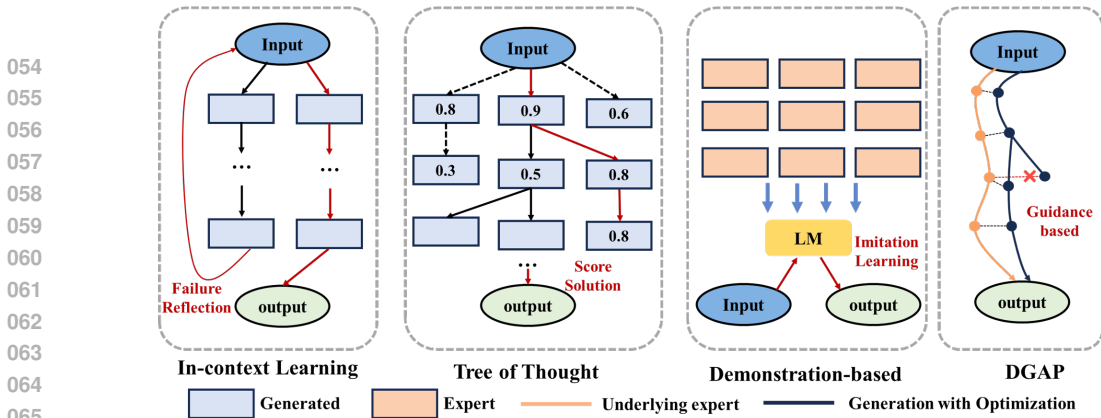


Figure 1: Comparing methods of LLMs to conduct embodied planning. DGAP leverages step-wise alignment signals to guide LLMs in the planning process.

challenge is applying the limited information from few-shot demonstrations in diverse scenarios. As described before, embodied agents that directly imitate these demonstrations often accumulate errors due to their restricted scope (Ross et al., 2011; Luo et al., 2024). In contrast, humans possess distinct capabilities for internal generalization and alignment (Barsalou, 2008; Rizzolatti & Craighero, 2004), allowing them to comprehend quickly task objectives and environment dynamics from few-shot demonstrations (Schaal, 1999; Malaviya et al., 2022). Motivated by this, we allow the agent to acquire a small number of demonstrations and further leverage them to provide step-wise signals to embodied planning. Specifically, (i) the demonstrations includes task objective and dynamics constraints that are lacking in LLMs, while it struggles to handle Out-Of-Distribution (OOD) situations across diverse scenarios; and in contrast, (ii) LLMs that contain a vast amount of commonsense knowledge enabling long-term reasoning on a broad set of situations without suffering from OOD problems, while LLMs lack domain knowledge and expert guidance for grounding. As a result, our work aims to combine the benefits of LLMs with the precise insights from demonstrations to provide few-shot generalization and task-specific grounding simultaneously.

In this paper, we propose a novel framework named Discriminator-Guided Action Optimization (DGAP) to perform efficient grounding and generalization for the LLM planner at every step. Instead of imitating expert actions, we learn a discriminator on a small number of demonstrations to form a score function within the framework of sentence transformers, which measures the alignment between LLM actions and underlying expert actions at the step level. By using meta-prompts that contain previously generated actions with score guidance Yao et al. (2023a), the LLM planner performs as a closed-loop optimizer for new actions with high scores through its understanding of existing discriminative action-score pairs. This approach effectively treats the LLM as an optimizer (Yang et al., 2024), which inherently involves an optimizing process, bypassing the need for physical or outcome feedback required by previous methods for refinement. Under mild conditions, we show that DGAP resembles the critic-regularized optimization in RL and is provable to achieve a stronger policy than the LLM planner.

Our contributions are summarized as follows. (i) We propose a novel framework that combines the long-term reasoning of LLMs and task-specific grounding under guidance from a small number of demonstrations. (ii) We propose a simple discriminator learned with a small number of demonstrations to serve as a step-level score function, which helps the LLM planner generate high-score actions via implicit optimization. (iii) We build theoretical connections between DGAP and critic-regularized optimization in RL, which shows our method obtains a stronger policy than the LLM planner under mild conditions. (iv) We conduct extensive experiments in challenging ScienceWorld (Wang et al., 2022) and VirtualHome (Puig et al., 2018) benchmarks combined with different LLM planners (GPT-4 (OpenAI, 2023), Llama3-70B (Meta, 2024)), and the result shows DGAP obtains superior performance and better efficiency than previous methods.

## 2 PRELIMINARIES

The embodied tasks can be formalized as a Markov Decision Process (MDP) defined by a tuple  $\mathcal{M} = (\mathcal{L}, \mathcal{S}, \mathcal{O}, E, \mathcal{A}, \mathcal{P}, r, T)$ . In the MDP,  $l \sim \mathcal{L}$  is the language description of a task specifying a high-level goal. For example, in ScienceWorld, a task description can be "your task is to boil lead"

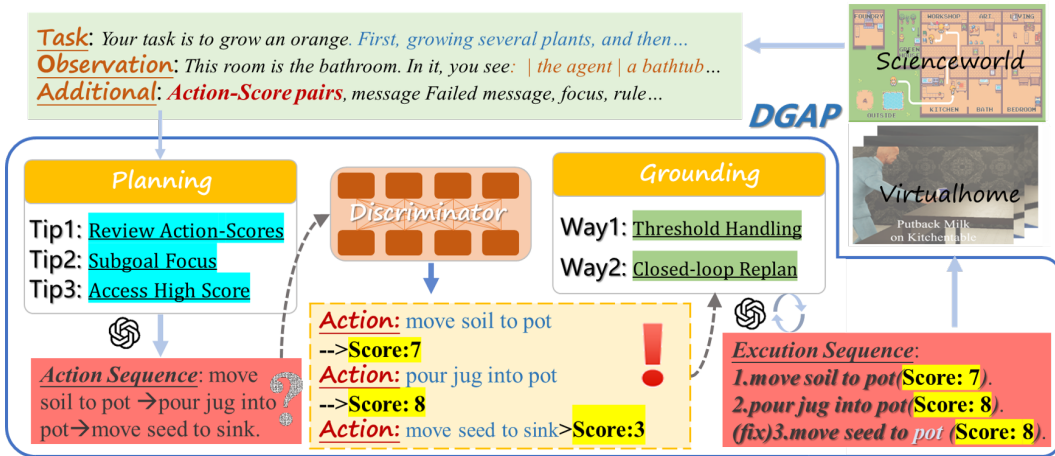


Figure 2: Framework of DGAP: (i) Acquiring domain-specific knowledge through discriminator’s regressive training. (ii) Optimizing action generation via historical action-score pairs.

At time step  $t$ , the state  $s_t \sim \mathcal{S}$  contains the description of environment information including the agent observations  $o_t \sim \mathcal{O}$  (i.e., environment feedback of previous action or information queried) and environment states  $e_t \sim \mathcal{E}$  (i.e., details about all visible objects). The action  $a_t \sim \pi(a|s_t)$  is generated by following a valid policy  $\pi : \mathcal{S} \rightarrow \Delta_{\mathcal{A}}$ . For example, an LLM planner  $\pi^{\text{llm}}(a_t|s_t)$  is a valid policy that generates an action  $a_t$  based on the state  $s_t$ . In most embodied planning tasks, a valid action should follow some supported action templates such as "use  $X$  on  $Y$ , examine  $Y$ ". For example, a valid action  $a_t$  in this task can be "use thermometer on liquid tin," and the initial action  $a_0$  is always "look around" for showing initial environment information. Each step involves the agent executing the action to interact with the environment, obtaining the next state  $s_{t+1}$  and some reward  $r_t$ . For an RL-based agent, the rewards will be used for policy learning via policy gradient algorithms. As for an LLM policy, the policy generates actions based on commonsense knowledge, the provided prompts, and (optionally) the closed-loop feedback.

In DGAP, we additionally acquire a small number of demonstrations, which include the optimal action sequences generated by an oracle planner  $\pi^{\text{oracle}}$ . We denote the expert dataset as  $\mathcal{B} = \{l, (a_0^i, a_1^i, \dots, a_T^i)\}_{i=1}^M$ , where  $M$  denotes the number of episodes. An imitation policy  $\pi^{\text{bc}}$  is learned via Behavior Cloning (BC) in the expert data, by maximizing the log-likelihood of expert actions as  $\pi^{\text{bc}} = \max_{\pi} \mathbb{E}_{\mathcal{B}}[\pi(a_t^i|l, h_t)]$ , where  $h_t = a_{t-1}^i, \dots, a_{t-n}^i$  contains previous actions up to 10.  $\pi^{\text{bc}}$  can perform poorly in real-world interactions due to limited state coverage of demonstrations.

### 3 METHOD

In this section, we present the details of our proposed framework, DGAP, as depicted in Fig. 2. This framework capitalizes on the domain knowledge embedded in both expert and handcrafted datasets to assign scores to responses from the LLM. These scores then strategically guide LLMs in planning towards specified objectives. Specifically, it consists of three parts: (i) Acquiring domain-specific knowledge through discriminator’s regressive training from augmented expert data with score labels in §3.1. (ii) Utilizing the pre-trained discriminator to optimize action generation via historical action-score pairs and ground actions when facing anomalous scores in §3.2. (iii) Qualitative analysis of DGAP and critic-regularized optimization.

#### 3.1 THE DISCRIMINATOR AS SCORER

As previously mentioned, reflection-based methods (Madaan et al., 2023; Shinn et al., 2023) and search-based methods (Yao et al., 2023a; Chen et al., 2024a; Zhou et al., 2023a) supervised by outcome present inefficient to some extent. Demonstration-based methods require large datasets for their scalability in embodied tasks (Rita et al., 2024; Sun & van der Schaar, 2024). Recognizing the potential complementarity of them, we investigate a solution that combines their strengths by em-

162 ploying a discriminator. Specifically, the discriminator integrates external knowledge from demon-  
 163 strations, subsequently provides a *score* measuring the alignment between the LLM’s response and  
 164 the underlying expert choice within the current context. The process is defined as:

$$165 \mathcal{D}_\phi : (l, h_t, a_{\pi^{\text{llm}}(l, s_t)}) \rightarrow Q, \quad (1)$$

166 where  $D_\phi$  denotes the offline discriminator with parameters  $\phi$ ,  $l, s_t$  refers to task objective and  
 167 environmental information as stated in Sec. 2,  $h_t$  is a summary of the past ten actions,  $a_{\pi^{\text{llm}}(l, s_t)}$   
 168 represents the action generated by LLM based on task goal and state at timestep  $t$ .  $Q$  is the score  
 169 (between 0 and 10), where a higher score indicates greater alignment with the expert policy. A  
 170 detailed description of the discriminator is in Appendix C.

171 Previous research has highlighted the generalization capacity and adaptability of demonstrations in  
 172 planning for various embodied tasks (Mu et al., 2023; Lin et al., 2023). Unlike existing methods that  
 173 directly utilize fixed demonstrations to transfer to new scenarios, our approach converts the demon-  
 174 strations’ information into numeric values, enabling a measurable step-level feedback. Additionally,  
 175 We enhance these values through augmentation on limited demonstration samples to improve their  
 176 generalization across embodied scenarios. This numeric representation is used to simplify integra-  
 177 tion with task planning, offering a more efficient, scalable solution with dense feedback.

178 **Data Overview** The discriminator is designed to numerically differentiate actions. Intuitively,  
 179 embedding regression serves as an effective method for this purpose. A predominant factor con-  
 180 tributing to this is the high similarity between expert action embeddings and those of generated  
 181 actions, which makes it difficult to distinguish and be represented as a score with generalization.  
 182 To tackle this issue, previous studies propose data distribution adjustments such as an unbalanced  
 183 combination of expert data, sub-optimal data (Xu et al., 2022), and data augmentation to provide  
 184 generalization (Jha et al., 2020) utilizing a customized fine-tuned LM (Tan et al., 2024). In light of  
 185 them, we adopt a data collection strategy that involves a tailored modification to expert data, com-  
 186 bined with comparable random data and a substantial volume of generated data via fine-tuned LM,  
 187 as illustrated in Fig. 3. And the specific implementing details are stated in Appendix. C.

- 189 • **Expert Data (score 10):** This parts are composed of oracle trajectories from ScienceWorld (Lin  
 190 et al., 2023) and VirtualHome (Puig et al., 2018) official datasets, from which we exact  $l$  and  $h_t$   
 191 as instructions. The correlated instruction-action pairs adhere to policy  $\pi^{\text{oracle}}$  and are assigned a  
 192 score of 10. Together, they constitute dataset  $\mathcal{B}_e$ .
- 193 • **Random Data (score 0):** We collect a dataset with negative pairs where the instruction is paired  
 194 with a ground truth action from demonstrations that is the least semantically related, where both  
 195 the predicate and the object of the action are changed and collectively form the dataset  $\mathcal{B}_r$ .
- 196 • **Offline Data (score within [0, 10]):** Accomplishing regression tasks using highly polarized sam-  
 197 ples presents considerable difficulty. To enrich the diversity of both instructions and actions, we  
 198 fine-tune a language model (LM) via imitation learning (IL) to provide domain knowledge, using  
 199 the instruction-action pairs in expert data, as detailed in Appendix B. Subsequently, we utilize a  
 200 fine-tuned model to generate action candidates  $a_{\pi^{\text{bc}}}$  through beam search across a range of instruc-  
 201 tions, thereby forming entirely new pairs. Here  $a_{\pi^{\text{bc}}}$  denotes the action generated by the fine-tuned  
 202 LM. We employ a pre-trained sentence embedding model to extract candidates’ features and fur-  
 203 ther evaluate semantic similarity with ground-truth actions  $a_{\pi^{\text{oracle}}}$ . This process is described as  
 204  $\text{Sim}(a_{\pi^{\text{bc}}}, a_{\pi^{\text{oracle}}})$ . In unseen scenarios without ground-truth, we mildly treat the first candidate  
 205 generated by the LM as 10 for the distribution of fine-tuned small models aligns more closely with  
 206 the training data domain (Panigrahi et al., 2023). The scores for the subsequent candidates are  
 207 determined by multiplying their cosine similarity to the first candidate by 10. These data hereby  
 make up dataset  $\mathcal{B}_a$  and constitute a significant proportion of the overall dataset  $\mathcal{B}_o$ .

208 The reason we transfer the similarity naturally ranges between  $[0, 1]$  to integrals between  $[0, 10]$  is  
 209 that LLMs more effectively process integers than decimals (Gruber et al., 2024). Thus, during the  
 210 discriminator’s training, we scaled the scores to span in  $[0, 10]$  and subsequently rounded them to  
 211 integers for the subsequent stage of LLM reasoning to better optimize LLMs’ interpretative effec-  
 212 tiveness.

213 **Model Overview** Previous research has demonstrated the significant capability of sentence trans-  
 214 formers in performing text classification (Cohan et al., 2019). Similarly, We also formulate our dis-  
 215 criminators’ training as a regression task and employ another sentence transformer-based network

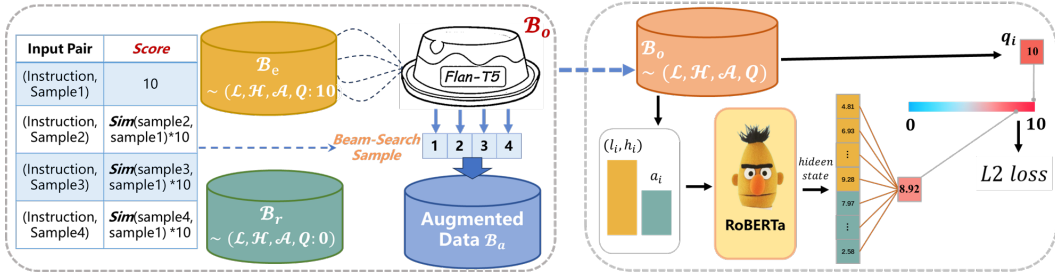


Figure 3: Illustration of dataset construction and discriminator training

as a backbone, utilizing the data in  $\mathcal{B}_o$ , which aims to establish the mapping from instruction-action pairs to scores. Specifically, we employ the RoBERTa (Liu et al., 2019) model architecture complemented by a linear head to get a precise score, thereby ensuring a robust integration of paired data into our evaluative framework. We explicitly apply L2 loss in training as shown in equation 2. Details are in Appendix C.

$$\mathcal{L} = \arg \min_{\phi} \left( \mathbb{E}_{(\mathcal{L}, \mathcal{H}, \mathcal{A}) \sim \mathcal{B}_o, \mathcal{A} \sim \pi^{\phi}} \left[ \sum_{i=1}^n \|\mathcal{D}_{\phi}(l_i, h_i, a_i) - Q_i\|_2 \right] \right) \quad (2)$$

The introduction of discriminator offers intuitive and readily obtainable feedback which supplants accessing feedback through exploration in the environment, and enhances the planning process by directly concentrating on the action-score information.

### 3.2 LLM OPTIMIZATION WITH DISCRIMINATOR

In this section, we outline how to combine the pre-trained discriminator with in-context learning to boost planning: (i) Prompts with scores to equip the LLM with the foresight to discern whether each action contributes to the successful completion of the task. (ii) Given the LLM’s inherent role as a sampler (Zhao et al., 2023a; Hopkins et al., 2023), a closed-loop feedback is introduced to ensure the optimization process. When the action score at any step falls below a predefined threshold, the LLM planner is required to adjust its policy in response to the suboptimal performance observed in the prior iteration.

**Prompt with scores** Unlike the prevalent use of Outcome-Supervised Prompts, which assess only the final outcome of solutions (Hu et al., 2023; Zhou et al., 2023a; Shinn et al., 2023; Yao et al., 2023b; Wang et al., 2023c), our approach implements a Process-Supervised Prompt (PSP) via scores obtained at each step.

Through this way, LLMs are encouraged to model and optimize task completion by evaluating intermediate steps, enhancing its decision-making in complex, long-term tasks (Hao et al., 2024; Xiong et al., 2024). Specifically, LLMs are allowed to see the entire trajectory of executed action-score pairs, dynamically adjusting its next action to maximize future rewards. By focusing the planning on numerical feedback, the approach is similar to reinforcement learning (RL), where agents refine their policies through incremental action-based rewards, as to identify key decision points, evaluate potential future paths, and rebalance its plan according to the stepwise feedback. There are more details in Corollary 3.2. The structured feedback mechanism ensures that each action aligns actions more accurately with long-term objectives while reducing the risk of cumulative errors (Sun & van der Schaar, 2024; Rita et al., 2024), a challenge aforementioned in embodied planning.

Building on this theoretical foundation, we integrate step-based scores into the prompt structure. Several studies have demonstrated that LLMs’ numerical sensitivity and utilization capabilities can be unveiled through appropriate prompting (Yang et al., 2024; Liu et al., 2023). Drawing inspiration from these findings, we have integrated the following context into our prompts to heighten

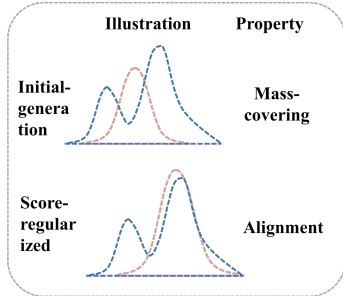


Figure 4: Regularizing the LLM policy distribution through score-based replanning

the model’s focus and faithfulness on scores and further leverage LLMs’ capacity to generate and optimize existing solutions. For a detailed prompt template, please refer to Appendix D.3.

*Previous actions, scores and observations are as follows...  
You are required to **maximize high-score actions cumulatively** while adhere to the task  
Identify the **intrinsic relationship** between the action-score pairs*

**Refinement for the failed plan** As an inherent role as a sampler (Zhao et al., 2023a; Hopkins et al., 2023), the LLM is required to function as an optimizer. Considering the difficulty of generating action by score maximizing implicitly and the hindrance caused by high variance in action-score pairs to the LLM, a closed-loop refinement process is introduced. If the score falls below the threshold  $\tau$ , the LLM is asked to replan based on the unsatisfactory action-score pair until  $D_\phi(l_t, h_t, a_t \sim \pi_{\text{llm}}) > \tau$ , as illustrated in Fig. 7. This ensures improvements over  $\pi_{\text{llm}}$  by score, with minimal changes to its policy through the closed-loop replanning process. It also decreases the interaction rounds of agents since the action  $a_t$  has been evaluated and refined via discriminator feedback before execution. Specifically, we adopt a threshold of 5 for ScienceWorld and 6 for VirtualHome, based on their respective training data distributions.

### 3.3 QUALITATIVE ANALYSIS

In the following, we give qualitative analysis to connect the proposed framework and the critic-regularized optimization problem. Since the score function  $\mathcal{D}_\phi(s, a)$  measures the similarity between LLM actions and expert actions, it forms an implicit *reward function* for the LLM agent as  $r_\phi = \mathcal{D}_\phi(s, a)$ . In DGAP, since the planner is prompted to generate an action that maximizes the score function, our method implicitly maximizes the reward considered in the RL framework. Meanwhile, since the output of DGAP largely relies on the commonsense knowledge of the initial LLM planner (i.e.,  $\pi^{\text{llm}}$ ), the resulting policy still lies closely to the  $\pi^{\text{llm}}$ . As a result, our method can be formalized as a constrained optimization problem that aims to learn an improved policy  $\pi^{\text{dgap}}$  over the initial  $\pi^{\text{llm}}$  by maximizing rewards, as

$$\pi^{\text{dgap}} = \arg \max_{\pi_\theta} \mathbb{E}_{s_t \sim d_{\text{llm}}^\pi, a_t \sim \pi^{\text{llm}}} \left[ \sum_t r_\phi(s_t, a_t) \right] - \beta D_{\text{KL}} [\pi_\theta(a_t | s_t) \| \pi^{\text{llm}}(a_t | s_t)], \quad (3)$$

where the states are sampled from a state distribution  $d_{\text{llm}}^\pi(s)$  induced by the LLM policy, the actions are sampled by following the LLM policy, and  $\beta$  is a balance factor. The cumulative return is defined as  $R_\phi(s_t, a_t) = \sum_{i=t}^{T-1} r_\phi(s_i, a_i)$  without a discount factor. Then the optimization objective becomes

$$\mathcal{L}^{\text{dgap}} = \mathbb{E}_{s \sim d_{\text{llm}}^\pi, a \sim \pi^{\text{llm}}} [R_\phi(s, a)] - \beta D_{\text{KL}} [\pi_\theta(a | s) \| \pi^{\text{llm}}(a | s)]. \quad (4)$$

In DGAP, since  $R_\phi(s, a)$  comes from a learned discriminator, it can be considered as the *critic* in an RL framework. We remark that such an objective is slightly different from DGAP where the LLM planner is prompted to generate actions that maximize the single-step return rather than the cumulative return since an episode-level discriminator can be more difficult to train. Nevertheless, for embodied planning tasks in ScienceWorld and VirtualHome, a successful multi-step plan requires single-step optimality in each planning step. The objective in equation 4 resembles a critic-regularized RL objective (Peng et al., 2019). Then the following Lemma gives the solution for  $\pi_\theta$  that maximizes this objective.

**Lemma 3.1.** *The optimal policy that solves the constrained optimization problem in  $\mathcal{L}^{\text{dgap}}$  is*

$$\pi_\theta^*(a | s) = \pi^{\text{llm}}(a | s) \exp(R_\phi(s, a) / \beta) / Z(s), \quad (5)$$

where  $Z(s)$  is a normalized factor to make  $\pi_\theta^*(a | s)$  a valid policy, i.e.,  $\int_a \pi_\theta^*(a | s) da = 1$ .

The proof is given in Appendix A. Then we have a direct corollary, which is as follows:

**Corollary 3.2.** *The updated policy  $\pi_\theta^*(a | s)$  improves over  $\pi^{\text{llm}}(a | s)$  as  $Q^{\pi_\theta^*}(s, a) \geq Q^{\pi^{\text{llm}}}(s, a)$ .*

The proof is given in Appendix A. In Corollary 3.2, the  $Q$ -function is defined as the expected return as  $Q^\pi(s, a) = \mathbb{E}_\pi [R_\phi(s, a)]$ . As a result, the policy  $\pi_\theta^*(a | s)$  is provable to obtain a higher expected

return than  $\pi^{\text{llm}}$  in the data coverage of the LLM policy. In practice,  $Z(s)$  is a partition function that can be hard to estimate, so we have

$$\pi^{\text{dgap}} \propto \pi^{\text{llm}}(a|s) \exp(R_\phi(s, a)/\beta). \quad (6)$$

Thus, the resulting policy  $\pi^{\text{dgap}}$  combines the benefits of the LLM planner and score function. Specifically, LLM is a basic policy that gives candidates actions with high probability, and then the score function forms a filter to choose actions from the candidates with the highest scores. Such a process is simplified in DGAP by using LLM as an optimizer, finally obtaining better policies in expected returns. The parameter  $\beta$  is a tuning factor that balances the effect of the LLM planner and score functions. In a special case, when  $\beta \rightarrow \infty$ , we have  $\pi_\theta^* \approx \pi^{\text{llm}}$ .

**Connection to RLHF.** Our method is also closely related to Reinforcement Learning from Human Feedback (RLHF) (Ouyang et al., 2022; Bai et al., 2022; Touvron et al., 2023), which follows a similar optimization objective as in equation 3 that optimizes some reward function with constraints to the supervised fine-tuning (SFT) model. However, there exist several major differences. (i) The rewards in DGAP are learned from demonstrations and sampled offline data, while in RLHF are learned from human preference data that can be more expensive to collect. (ii) The reward function in DGAP is trained by a simple regression objective, while RLHF requires BT-model for explicit reward learning or DPO-style optimization for implicit reward learning (Lambert et al., 2024). (iii) We consider LLM itself as an optimizer via interactive prompting, while RLHF requires explicit optimization via RL (Ahmadian et al., 2024) or DPO (Rafailov et al., 2024) by updating the parameters of LLMs. Thus, our method is desirable for API-based strong LLM models, while RLHF often requires an open-sourced LLM model for reward learning and RL optimization.

## 4 RELATED WORK

**Embodied Planning with LLMs** LLMs have exhibited notable reasoning abilities in solving various tasks through in-context examples and prompting techniques like chain-of-thought (Wei et al., 2022; Vemprala et al., 2023) and tree-of-thought (Yao et al., 2023a; Zhou et al., 2023a; Feng et al., 2023). However, for embodied tasks, the in-context learning often fails as the embodied knowledge is lacking or even conflicts with that in LLMs. The existing methods introduce closed-loop feedback such as self-reflection mechanisms for self-evaluation and re-plan based on failure analysis (Madaan et al., 2023; Huang et al., 2022a; Yao et al., 2023b; Chen et al., 2024a), and external feedback for reflection (Shinn et al., 2023; Mandi et al., 2023; Zhou et al., 2023b), making them considerably costly and inefficient in querying or interactions. In contrast, we learn score function from demonstrations, eliminating the reliance on self-evaluation and external feedback. Several methods have recently considered LLMs as RL agents that can interact with the environment to collect transitions with external rewards, and perform parameter tuning by RL algorithms (Yao et al., 2024; Zhai et al., 2024). In contrast, our method is designed for API-based LLMs without parameter tuning. Similar to use, SwiftSage (Lin et al., 2023) adopts demonstrations in LLM planning while relying on imitation learning to generate actions. In contrast, we train a score function from demonstrations with augmented data, which leads to a new solution to combine the benefits of LLMs and demonstrations.

**LLM for Decision Making.** Beyond planning, LLMs can also play other important roles in embodied decision-making. (i) LLMs as a reward designer (Ma et al., 2023; Xie et al., 2023; Yu et al., 2023). The code-writing ability of LLMs can be used to generate reward codes according to the robot and task scripts. The reward function is used to train an RL policy, and the feedback from the environment can be used to perform evolutionary optimization for code generation. (ii) LLMs as a world model (Zhao et al., 2023b; Hao et al., 2023; Murthy et al., 2023). The world model is important for predicting future states and simulating long-term outcomes of actions. LLM can serve as a world model that benefits model-based RL and LLM planning. (iii) LLMs a foundation policy. LLMs can serve as a policy for imitation learning (Li et al., 2024; Brohan et al., 2023), and the policy is fine-tuned with embodied data from real-world tasks. (iv) LLM as codes generator. LLM can directly generate robot code for execution (Liang et al., 2023; Mu et al., 2024) or generate value maps to combine with model-predictive control methods (Huang et al., 2023). (v) Environment generator. LLMs can generate environments and tasks in a simulator via a closed-loop process (Wang et al., 2023a;b), which can subsequently generate training data for policy learning.

Task Type	*Len	TDT	SFT	Reflexion	S-GPT4	D-GPT4	S-Llama3	D-Llama3
1-1(L)	107.70	0.71	15.00	4.22	97.04	<b>100.00</b>	40.33	<b>82.67</b>
1-2(L)	78.60	0.44	24.40	10.61	87.04	<b>92.75</b>	79.00	<b>91.50</b>
1-3(L)	88.90	3.88	32.20	7.78	72.78	<b>74.00</b>	59.33	<b>82.67</b>
1-4(L)	75.20	0.55	57.45	0.92	100.00	<b>100.00</b>	84.00	<b>90.66</b>
2-1(M)	21.40	6.16	9.45	5.92	99.17	<b>100.00</b>	76.00	<b>78.67</b>
2-2(M)	35.20	6.43	6.75	28.59	<b>88.17</b>	80.17	<b>58.00</b>	46.67
2-3(L)	65.00	19.87	5.75	22.37	<b>95.73</b>	88.33	76.00	<b>76.00</b>
3-1(S)	13.60	40.55	70.00	<b>100.00</b>	88.67	<b>91.50</b>	76.00	<b>78.67</b>
3-2(M)	20.80	14.26	48.33	17.45	55.33	<b>58.00</b>	100.00	<b>100.00</b>
3-3(M)	25.60	10.16	59.50	72.54	71.90	<b>78.57</b>	100.00	<b>100.00</b>
3-4(M)	29.00	21.65	69.00	70.22	77.86	<b>88.14</b>	100.00	<b>100.00</b>
4-1(S)	14.60	41.93	<b>100.00</b>	64.93	100.00	<b>100.00</b>	100.00	<b>100.00</b>
4-2(S)	8.80	55.76	<b>100.00</b>	87.27	100.00	<b>100.00</b>	100.00	<b>100.00</b>
4-3(S)	12.60	27.82	94.45	16.42	91.67	<b>100.00</b>	72.33	<b>76.29</b>
4-4(S)	14.60	47.15	<b>100.00</b>	<b>100.00</b>	100.00	<b>100.00</b>	100.00	<b>100.00</b>
5-1(L)	69.50	6.89	13.45	7.33	<b>74.59</b>	73.14	58.00	<b>78.00</b>
5-2(L)	79.60	11.86	44.67	13.00	<b>93.93</b>	90.57	35.67	<b>57.33</b>
6-1(M)	33.60	15.10	26.25	<b>70.35</b>	49.40	<b>57.40</b>	<b>100.00</b>	78.67
6-2(S)	15.10	15.70	53.33	70.67	100.00	<b>100.00</b>	100.00	<b>100.00</b>
6-3(M)	23.00	5.25	8.00	15.77	91.48	<b>92.43</b>	<b>84.67</b>	68.00
7-1(S)	7.00	30.00	11.19	<b>100.00</b>	95.00	<b>100.00</b>	<b>100.00</b>	85.71
7-2(S)	7.00	8.43	83.33	67.50	85.00	<b>85.71</b>	84.67	<b>92.00</b>
7-3(S)	8.00	8.34	<b>100.00</b>	50.00	<b>93.33</b>	92.71	80.00	<b>100.00</b>
8-1(M)	40.00	3.86	77.87	2.58	89.00	<b>100.00</b>	52.00	<b>100.00</b>
8-2(S)	16.30	8.00	33.00	8.00	<b>68.50</b>	38.50	<b>61.67</b>	45.00
9-1(L)	97.00	2.53	8.00	50.63	75.00	<b>75.00</b>	50.00	<b>57.14</b>
9-2(L)	84.90	14.66	73.33	<b>100.00</b>	70.00	<b>83.33</b>	66.67	<b>100.00</b>
9-3(L)	123.10	9.12	<b>73.33</b>	70.62	60.00	<b>71.43</b>	77.67	<b>88.67</b>
10-1(L)	130.10	1.51	53.33	50.90	<b>92.30</b>	87.71	43.00	<b>53.00</b>
10-2(L)	132.10	1.29	17.00	23.69	77.60	<b>78.00</b>	78.00	<b>84.00</b>
Short	11.76	28.37	78.68	71.47	<b>92.22</b>	90.84	87.47	<b>87.77</b>
Medium	28.58	10.36	32.90	35.43	77.79	<b>81.84</b>	83.83	<b>84.01</b>
Long	94.30	6.11	32.55	30.17	83.00	<b>84.52</b>	62.31	<b>78.47</b>
Overall	49.26	14.66	49.22	45.34	84.68	<b>85.91</b>	76.43	<b>82.96</b>

Table 1: TASK PERFORMANCE ACROSS BASELINES IN SCIENCEWORLD.

## 5 EXPERIMENTS

To evaluate the effectiveness of DGAP and other baseline methods in complex embodied reasoning tasks, we employ the ScienceWorld (Wang et al., 2022) and VirtualHome (Puig et al., 2018) benchmark. They both encompass a collection of open scenarios and diverse objects for manipulation to accomplish embodied tasks.

### 5.1 SCIENCEWORLD

**Experimental Setup** We conducted our evaluation on ScienceWorld, a virtual textual environment designed for complex science tasks that are structured with 30 different types of science experiments across 10 topics, featuring diverse locations like an art studio, kitchen, and outdoor area. Over 200 types of interactive objects and 25 action templates are included.

Our evaluation employed a series of test variations that presented unique combinations of objects and scenarios. For example, while our expert data included experiments such as freeze water, the evaluation extended to scenarios requiring the freeze mercury.

**Compared Methods** We benchmark DGAP methodology against three kinds of approaches: (i) **Behavior Cloning-Only**: The Text Decision Transformer (TDT) leverages behavior cloning and incorporates reward-to-go as an input, which enables the model to predict actions designed to maximize future expected rewards (Chen et al., 2021). (ii) **Planning via Self-Reflection**: Techniques such as Reflexion (Shinn et al., 2023) integrate a self-reasoning mechanism within the planning pro-



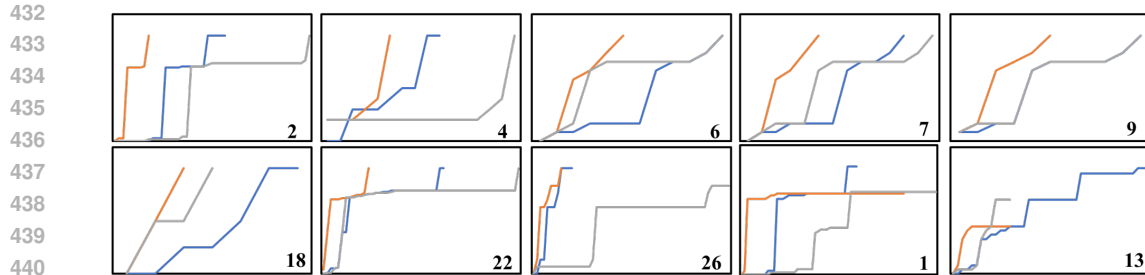


Figure 5: Visualizing trajectories of **DGAP**, **SWIFTSAGE** and **ORACLE**,  $X$ : time steps,  $Y$ : scores. Task identifiers are positioned at the bottom right of each figure, whose detailed information can be found in Fig. 10.

cess to enhance reasoning capabilities. **(iii) Demonstration Method:** STF is based on imitation learning on expert data. SwiftSage (Lin et al., 2023) amalgamates rapid thinking with demonstrations as our method and methodical reasoning, establishing itself as the state-of-the-art baseline in ScienceWorld, making it our primary focus of compare.

For our implementations, We used around around half number of demonstrations as ToT, SFT, and SwiftSage, with 10 to 30 trajectories per task. For Reflexion, we provided the three most relevant trajectories in the context each time, ensuring coverage of expert trajectories across tasks. We utilize Llama3-70B and GPT-4 as the foundational Large Language Models. Specifically, **S-GPT4** represents the SwiftSage method utilizing GPT-4, while **D-GPT4** denotes the DGAP strategy integrated with GPT-4. Similarly, **S-Llama3** corresponds to the SwiftSage approach adapted Llama3-70B, and **D-Llama3** signifies the DGAP method deployed with Llama3-70B. TDT and Reflexion utilize GPT-4.

**Results** Our findings are outlined in Tab. 5.1, which elucidates the performance across thirty distinct task types. The details of tasks can be referred in Appendix. 3. Analysis of the results yields several observations: **(i)** DGAP outperforms SwiftSage in most tasks, suggesting that the external suggestion of alignment with expert data is more effective than limited internal environmental feedback. **(ii)** In tasks classified as **short**, our method shows no substantial superiority over SwiftSage. We suspect this comes from the limited pairs of short task sequences being less effective compared to the plentiful pairs in long trajectories, while short tasks primarily rely on detailed textual information to elicitate LLMs’ reasoning prowess. **(iii)** In addition to the success rate, DGAP demonstrates a notable enhancement in efficiency, achieving higher scores in fewer steps as validated by external expert assessments. This increased efficiency is visually represented in Fig. 5 and in Appendix 10. **(iv)** The inferential prowess of various LLMs exhibits discrepancies, with each excelling in distinct areas. For example, GPT-4 shows outstanding performance in tasks 1-1, 1-3, and 1-4, which involve changing the state of objects. Conversely, in more complex scenarios such as tasks 3-3, 3-4, and 3-5 that are related to circuits, Llama3 surpasses GPT-4, underscoring the diverse strengths of different models.

## 5.2 VIRTUALHOME

**Experimental Setup** VirtualHome is an interactive platform to simulate complex household activities via programs and train agents to perform complete them. It also includes a Knowledge Base, Providing instructions for a diverse combination of activities, such as *put one pancake in stove and switch on stove, put two milk on kitchentable*.

We perform experimental evaluations on three distinct settings as delineated in (Li et al., 2022): **In-Distribution**, **NovelTasks**, and **NovelScenes**. They differ markedly in task complexity, which we assess using the number of action steps required for each task. Specifically, the average action steps required for **In-Distribution** are 13.4, for **NovelTasks** 25.61, and for **NovelScenes** 27.11. To ensure robustness and reliability of our findings, we replicate experiments on 60 tasks from each setting three times, thereby gathering comprehensive results. We employ **EXEC**. and **SR**. to evaluate the feasibility of the generated plans, where **EXEC**. measures whether the generated plan can be executed in the given environment, and **SR**. measures the fulfillment of task-specific goal conditions.

**Compared Methods** We evaluate DGAP against three kinds of approaches: **(i) Planning based:** LLMs employ a method that directly generates planning results through in-context learning, such as

	In-Distribution		NovelScenes		NovelTasks	
	EXEC.	SR.	EXEC.	SR.	EXEC.	SR.
<b>ProgPrompt</b>	87.33 ± 2.02	82.33 ± 1.76	38.67 ± 1.45	32.33 ± 1.45	49.67 ± 3.18	49.00 ± 3.21
<b>Inner Monologue</b>	79.67 ± 3.38	79.33 ± 3.18	54.33 ± 1.76	53.33 ± 1.76	47.33 ± 1.67	46.00 ± 1.15
<b>Tree Planner</b>	-	-	<b>89.33 ± 0.17</b>	41.67 ± 3.20	<b>90.33 ± 0.32</b>	52.33 ± 2.03
<b>DGAP-Llama3</b>	90.67 ± 0.86	84.33 ± 2.12	63.00 ± 1.68	56.33 ± 1.12	78.33 ± 1.03	68.00 ± 2.03
<b>DGAP-GPT4</b>	<b>93.33 ± 1.76</b>	<b>88.00 ± 2.45</b>	71.67 ± 1.15	<b>62.67 ± 1.33</b>	73.67 ± 1.15	<b>72.17 ± 3.18</b>
<b>DGAP-InternVL2-8B</b>	84.33 ± 1.15	68.67 ± 2.30	57.06 ± 2.11	45.33 ± 1.20	52.25 ± 1.00	41.17 ± 2.80

Table 2: OVERALL PERFORMANCE DGAP AND BASELINES ACROSS VIRTUALHOME

ProgPrompt (Singh et al., 2023). **(ii) Reasoning based:** In this approach, LLMs are rendered with a specialized prompting mechanism to enhance their inference when tackling complex tasks, such as Inner Monologue (Huang et al., 2022b). **(iii) Search based:** This approach reframes the inference process into plan sampling and tree construction, thereby establishing a comprehensive and efficient pathway for task execution (Hu et al., 2023). **(iii) VLM experiments:** We have supplemented our experiments with Vision Language Models (VLMs) in the VirtualHome benchmark. Specifically, we utilized InternVL2-8B to generate the key object states within scenes, replacing the information that was previously obtained directly from the environment graph. Additionally, due to the limitations of the VLMs’ field of vision, which only allows for the retrieval of objects within the current scene, we adjusted the action step length for each query. Instead of generating a full sequence for a subgoal at once, the generation now stops when the next action is [walk] (indicating a need to move to a different location) and then begin another in the new scene.

**Results** The "In-Distribution" task category is ill-suited to the Tree Planner (Hu et al., 2023) mechanism, designed to adapt to novel scene and task combinations. So, the experiments with Tree Planner in the In-Distribution setting are ignored. As shown in Tab. 8, the primary results emphasize several specific insights: **(i)** Across nearly all evaluated metrics and settings, DGAP consistently outperforms competing methodologies. This underscores the superior guidance our approach offers over environmental feedback, thereby significantly boosting success rates. **(ii)** In the majority of settings, DGAP demonstrates a minimal standard deviation. This indicates that our framework augments the embodied capabilities of LLMs and substantially improves their stability and robustness. **(iii)** Though the Tree Planner exhibits superior performance in EXEC. Due to the action tree being grounded and optimized, our method maintains a lead in success rates. This advantage stems from our continuous action evaluation loop, which refines the strategic foresight of LLMs by leveraging step-wise action-score pairs and real-time contextual inputs. **(iv)** The results indicate a relatively mild impact of using VLMs on action executability (EXEC) and a more significant influence on task success rate (SR). This suggests EXEC may rely more heavily on reasoning models rather than perception models, while SR appears to be more sensitive to the accuracy of environmental information. Additionally, we observe that among the three task categories, In-Distribution tasks are less affected by VLM-generated information, while the other two categories experience a greater impact. This suggests that familiar tasks exhibit a certain level of robustness under varying types of environmental descriptions.

Empirical evidence from experiments on two benchmarks corroborates that the DGAP method not only refines the performance of LLMs but also reduces the necessary steps and queries, thereby enhancing the efficiency and effectiveness of the embodied task’s planning process.

## 6 CONCLUSION

This paper presents the Discriminator-Guided Action Optimization (DGAP) framework, addressing the challenges of complex embodied tasks which demand extensive, executable planning in dynamic scenerios. By utilizing a few demonstrations, the DGAP framework establishes a discriminator with a scoring function as real-time feedback, guiding LLMs to closely align with expert actions. Experimental results demonstrate that DGAP outperforms other baseline methods in benchmarks such as ScienceWorld and VirtualHome, showcasing superior performance and higher efficiency. The limitations of this work lie in its suboptimal performance on short-sequence tasks and the additional effort required to prepare the data. In the future, We will also investigate lightweight frameworks and adopt a generalized approach to extend their applicability to a broader range of LLM tasks.

540  
541  
542  
543  
544  
545  
546  
547  
548  
549  
550  
551  
552  
553  
554  
555  
556  
557  
558  
559  
560  
561  
562  
563  
564  
565  
566  
567  
568  
569  
570  
571  
572  
573  
574  
575  
576  
577  
578  
579  
580  
581  
582  
583  
584  
585  
586  
587  
588  
589  
590  
591  
592  
593

## CODE OF ETHICS AND ETHICS STATEMENT

The research conducted in this paper adhere to, in every respect, with ICLR Code of Ethics (<https://iclr.cc/public/CodeOfEthics>).

This research adheres strictly to ethical guidelines, with all datasets handled appropriately concerning privacy and consent, and all participant data anonymized. We have evaluated the representativeness of the models and datasets to ensure fairness and have taken steps to minimize potential bias. Furthermore, the outcomes of this research will not be used to promote applications that could harm individuals, society, or the environment, particularly in areas such as safety, discrimination, or surveillance. Compliance with relevant laws and regulations is ensured.

## REPRODUCIBILITY

To ensure reproducibility, the code for our experiments is available at <https://anonymous.open.science/r/DGAP-5075/>. Detailed information on models, data processing steps and experiments can be found there.

## REFERENCES

- 594  
595  
596 Jacob Abernethy, Alekh Agarwal, Teodor V Marinov, and Manfred K Warmuth. A mechanism for  
597 sample-efficient in-context learning for sparse retrieval tasks. *arXiv preprint arXiv:2305.17040*,  
598 2023.
- 599  
600 Arash Ahmadian, Chris Cremer, Matthias Gallé, Marzieh Fadaee, Julia Kreutzer, Ahmet Üstün, and  
601 Sara Hooker. Back to basics: Revisiting reinforce style optimization for learning from human  
602 feedback in llms. *arXiv preprint arXiv:2402.14740*, 2024.
- 603  
604 Ekin Akyürek, Dale Schuurmans, Jacob Andreas, Tengyu Ma, and Denny Zhou. What learning  
605 algorithm is in-context learning? investigations with linear models. In *International Conference  
606 on Learning Representations*, 2023.
- 607  
608 Yuntao Bai, Andy Jones, Kamal Ndousse, Amanda Askell, Anna Chen, Nova DasSarma, Dawn  
609 Drain, Stanislav Fort, Deep Ganguli, Tom Henighan, et al. Training a helpful and harmless  
610 assistant with reinforcement learning from human feedback. *arXiv preprint arXiv:2204.05862*,  
611 2022.
- 612  
613 Lawrence W Barsalou. Grounded cognition. *Annu. Rev. Psychol.*, 59(1):617–645, 2008.
- 614  
615 Anthony Brohan, Noah Brown, Justice Carbajal, Yevgen Chebotar, Xi Chen, Krzysztof Choro-  
616 manski, Tianli Ding, Danny Driess, Avinava Dubey, Chelsea Finn, Pete Florence, Chuyuan Fu,  
617 Montse Gonzalez Arenas, Keerthana Gopalakrishnan, Kehang Han, Karol Hausman, Alexander  
618 Herzog, and et al. RT-2: vision-language-action models transfer web knowledge to robotic con-  
619 trol. *CoRR*, abs/2307.15818, 2023.
- 620  
621 Lili Chen, Kevin Lu, Aravind Rajeswaran, Kimin Lee, Aditya Grover, Misha Laskin, Pieter Abbeel,  
622 Aravind Srinivas, and Igor Mordatch. Decision transformer: Reinforcement learning via sequence  
623 modeling. *Advances in neural information processing systems*, 34:15084–15097, 2021.
- 624  
625 Sijia Chen, Baochun Li, and Di Niu. Boosting of thoughts: Trial-and-error problem solving with  
626 large language models. In *The Twelfth International Conference on Learning Representations*,  
627 2024a. URL <https://openreview.net/forum?id=qBL04XXex6>.
- 628  
629 Zehui Chen, Kuikun Liu, Qiuchen Wang, Wenwei Zhang, Jiangning Liu, Dahua Lin, Kai Chen, and  
630 Feng Zhao. Agent-flan: Designing data and methods of effective agent tuning for large language  
631 models. *arXiv preprint arXiv:2403.12881*, 2024b.
- 632  
633 Hyung Won Chung, Le Hou, Shayne Longpre, Barret Zoph, Yi Tay, William Fedus, Yunxuan Li,  
634 Xuezhi Wang, Mostafa Dehghani, Siddhartha Brahma, et al. Scaling instruction-finetuned lan-  
635 guage models. *Journal of Machine Learning Research*, 25(70):1–53, 2024.
- 636  
637 Arman Cohan, Iz Beltagy, Daniel King, Bhavana Dalvi, and Daniel S Weld. Pretrained language  
638 models for sequential sentence classification. *arXiv preprint arXiv:1909.04054*, 2019.
- 639  
640 Qingxiu Dong, Lei Li, Damai Dai, Ce Zheng, Zhiyong Wu, Baobao Chang, Xu Sun, Jingjing Xu,  
641 and Zhifang Sui. A survey for in-context learning. *arXiv preprint arXiv:2301.00234*, 2022.
- 642  
643 Xidong Feng, Ziyu Wan, Muning Wen, Ying Wen, Weinan Zhang, and Jun Wang. Alphazero-  
644 like tree-search can guide large language model decoding and training. *arXiv preprint  
645 arXiv:2309.17179*, 2023.
- 646  
647 Nate Gruver, Marc Finzi, Shikai Qiu, and Andrew G Wilson. Large language models are zero-shot  
time series forecasters. *Advances in Neural Information Processing Systems*, 36, 2024.
- 648  
649 Shibo Hao, Yi Gu, Haodi Ma, Joshua Jiahua Hong, Zhen Wang, Daisy Zhe Wang, and Zhiting Hu.  
Reasoning with language model is planning with world model. *arXiv preprint arXiv:2305.14992*,  
2023.
- 650  
651 Shibo Hao, Yi Gu, Haotian Luo, Tianyang Liu, Xiyan Shao, Xinyuan Wang, Shuhua Xie, Haodi  
Ma, Adithya Samavedhi, Qiyue Gao, et al. Llm reasoners: New evaluation, library, and analysis  
of step-by-step reasoning with large language models. *arXiv preprint arXiv:2404.05221*, 2024.

- 648 Aspen K Hopkins, Alex Renda, and Michael Carbin. Can llms generate random numbers? evaluat-  
649 ing llm sampling in controlled domains. In *ICML 2023 Workshop: Sampling and Optimization in*  
650 *Discrete Space*, 2023.
- 651 Mengkang Hu, Yao Mu, Xinmiao Yu, Mingyu Ding, Shiguang Wu, Wenqi Shao, Qiguang Chen,  
652 Bin Wang, Yu Qiao, and Ping Luo. Tree-planner: Efficient close-loop task planning with large  
653 language models. *arXiv preprint arXiv:2310.08582*, 2023.
- 654 Wenlong Huang, Fei Xia, Ted Xiao, Harris Chan, Jacky Liang, Pete Florence, Andy Zeng, Jonathan  
655 Tompson, Igor Mordatch, Yevgen Chebotar, Pierre Sermanet, Tomas Jackson, Noah Brown, Linda  
656 Luu, Sergey Levine, Karol Hausman, and brian ichter. Inner monologue: Embodied reasoning  
657 through planning with language models. In *Annual Conference on Robot Learning*, 2022a.
- 658 Wenlong Huang, Fei Xia, Ted Xiao, Harris Chan, Jacky Liang, Pete Florence, Andy Zeng, Jonathan  
659 Tompson, Igor Mordatch, Yevgen Chebotar, et al. Inner monologue: Embodied reasoning through  
660 planning with language models. *arXiv preprint arXiv:2207.05608*, 2022b.
- 661 Wenlong Huang, Chen Wang, Ruohan Zhang, Yunzhu Li, Jiajun Wu, and Li Fei-Fei. Voxposer:  
662 Composable 3d value maps for robotic manipulation with language models. In *Annual Conference*  
663 *on Robot Learning*, 2023.
- 664 Rohan Jha, Charles Lovering, and Ellie Pavlick. Does data augmentation improve generalization in  
665 nlp? *arXiv preprint arXiv:2004.15012*, 2020.
- 666 Nathan Lambert, Valentina Pyatkin, Jacob Morrison, LJ Miranda, Bill Yuchen Lin, Khyathi Chandu,  
667 Nouha Dziri, Sachin Kumar, Tom Zick, Yejin Choi, et al. Rewardbench: Evaluating reward  
668 models for language modeling. *arXiv preprint arXiv:2403.13787*, 2024.
- 669 Shuang Li, Xavier Puig, Chris Paxton, Yilun Du, Clinton Wang, Linxi Fan, Tao Chen, De-An Huang,  
670 Ekin Akyürek, Anima Anandkumar, et al. Pre-trained language models for interactive decision-  
671 making. *Advances in Neural Information Processing Systems*, 35:31199–31212, 2022.
- 672 Xinghang Li, Minghuan Liu, Hanbo Zhang, Cunjun Yu, Jie Xu, Hongtao Wu, Chilam Cheang,  
673 Ya Jing, Weinan Zhang, Huaping Liu, Hang Li, and Tao Kong. Vision-language foundation  
674 models as effective robot imitators. In *The Twelfth International Conference on Learning Repre-*  
675 *sentations*, 2024. URL <https://openreview.net/forum?id=1FYj0oibGR>.
- 676 Jacky Liang, Wenlong Huang, Fei Xia, Peng Xu, Karol Hausman, Brian Ichter, Pete Florence,  
677 and Andy Zeng. Code as policies: Language model programs for embodied control. In *IEEE*  
678 *International Conference on Robotics and Automation*, pp. 9493–9500. IEEE, 2023.
- 679 Bill Yuchen Lin, Yicheng Fu, Karina Yang, Faeze Brahman, Shiyu Huang, Chandra Bhagavatula,  
680 Prithviraj Ammanabrolu, Yejin Choi, and Xiang Ren. Swiftsage: A generative agent with fast and  
681 slow thinking for complex interactive tasks. In *Neural Information Processing Systems*, 2023.
- 682 An Liu, Zonghan Yang, Zhenhe Zhang, Qingyuan Hu, Peng Li, Ming Yan, Ji Zhang, Fei Huang, and  
683 Yang Liu. Panda: Preference adaptation for enhancing domain-specific abilities of llms. *arXiv*  
684 *preprint arXiv:2402.12835*, 2024.
- 685 Shengcai Liu, Caishun Chen, Xinghua Qu, Ke Tang, and Yew-Soon Ong. Large language models  
686 as evolutionary optimizers. *arXiv preprint arXiv:2310.19046*, 2023.
- 687 Yinhan Liu, Myle Ott, Naman Goyal, Jingfei Du, Mandar Joshi, Danqi Chen, Omer Levy, Mike  
688 Lewis, Luke Zettlemoyer, and Veselin Stoyanov. Roberta: A robustly optimized bert pretraining  
689 approach. *arXiv preprint arXiv:1907.11692*, 2019.
- 690 Jianlan Luo, Perry Dong, Yuexiang Zhai, Yi Ma, and Sergey Levine. Rlif: Interactive imitation  
691 learning as reinforcement learning. In *The Twelfth International Conference on Learning Repre-*  
692 *sentations*, 2024. URL <https://openreview.net/forum?id=oLLZhbBSOU>.
- 693 Yecheng Jason Ma, William Liang, Guanzhi Wang, De-An Huang, Osbert Bastani, Dinesh Jayara-  
694 man, Yuke Zhu, Linxi Fan, and Anima Anandkumar. Eureka: Human-level reward design via  
695 coding large language models. *CoRR*, abs/2310.12931, 2023.
- 700  
701

- 702 Aman Madaan, Niket Tandon, Prakhar Gupta, Skyler Hallinan, Luyu Gao, Sarah Wiegrefe, Uri  
703 Alon, Nouha Dziri, Shrimai Prabhumoye, Yiming Yang, et al. Self-refine: Iterative refinement  
704 with self-feedback. *arXiv preprint arXiv:2303.17651*, 2023.
- 705  
706 Maya Malaviya, Ilya Sucholutsky, Kerem Oktar, and Thomas L Griffiths. Can humans do less-than-  
707 one-shot learning? In *44th Annual Meeting of the Cognitive Science Society: Cognitive Diversity*,  
708 *CogSci 2022*, 2022.
- 709 Zhao Mandi, Shreya Jain, and Shuran Song. Roco: Dialectic multi-robot collaboration with large  
710 language models. *CoRR*, abs/2307.04738, 2023.
- 711  
712 Meta. Meta llama 3, <https://llama.meta.com/llama3>, 2024.
- 713 Yao Mu, Qinglong Zhang, Mengkang Hu, Wenhai Wang, Mingyu Ding, Jun Jin, Bin Wang, Jifeng  
714 Dai, Yu Qiao, and Ping Luo. EmbodiedGPT: Vision-language pre-training via embodied chain of  
715 thought. In *Neural Information Processing Systems*, 2023.
- 716  
717 Yao Mu, Junting Chen, Qinglong Zhang, Shoufa Chen, Qiaojun Yu, Chongjian Ge, Runjian Chen,  
718 Zhixuan Liang, Mengkang Hu, Chaofan Tao, Peize Sun, Haibao Yu, Chao Yang, Wenqi Shao,  
719 Wenhai Wang, Jifeng Dai, Yu Qiao, Mingyu Ding, and Ping Luo. Robocodex: Multimodal code  
720 generation for robotic behavior synthesis. *ArXiv*, abs/2402.16117, 2024. URL <https://api.semanticscholar.org/CorpusID:267938053>.
- 721  
722 Rithesh Murthy, Shelby Heinecke, Juan Carlos Nieves, Zhiwei Liu, Le Xue, Weiran Yao, Yihao  
723 Feng, Zeyuan Chen, Akash Gokul, Devansh Arpit, et al. Rex: Rapid exploration and exploitation  
724 for ai agents. *arXiv preprint arXiv:2307.08962*, 2023.
- 725  
726 OpenAI. Gpt-4 technical report, 2023.
- 727  
728 Long Ouyang, Jeffrey Wu, Xu Jiang, Diogo Almeida, Carroll Wainwright, Pamela Mishkin, Chong  
729 Zhang, Sandhini Agarwal, Katarina Slama, Alex Ray, et al. Training language models to fol-  
730 low instructions with human feedback. *Advances in neural information processing systems*, 35:  
731 27730–27744, 2022.
- 732  
733 Abhishek Panigrahi, Nikunj Saunshi, Haoyu Zhao, and Sanjeev Arora. Task-specific skill local-  
734 ization in fine-tuned language models. In *International Conference on Machine Learning*, pp.  
735 27011–27033. PMLR, 2023.
- 736  
737 Xue Bin Peng, Aviral Kumar, Grace Zhang, and Sergey Levine. Advantage-weighted regression:  
738 Simple and scalable off-policy reinforcement learning. *CoRR*, abs/1910.00177, 2019.
- 739  
740 Xavier Puig, Kevin Ra, Marko Boben, Jiaman Li, Tingwu Wang, Sanja Fidler, and Antonio Tor-  
741 ralba. Virtualhome: Simulating household activities via programs. In *Proceedings of the IEEE*  
742 *conference on computer vision and pattern recognition*, pp. 8494–8502, 2018.
- 743  
744 Rafael Rafailov, Archit Sharma, Eric Mitchell, Christopher D Manning, Stefano Ermon, and Chelsea  
745 Finn. Direct preference optimization: Your language model is secretly a reward model. *Advances*  
746 *in Neural Information Processing Systems*, 36, 2024.
- 747  
748 Mathieu Rita, Florian Strub, Rahma Chaabouni, Paul Michel, Emmanuel Dupoux, and Olivier  
749 Pietquin. Countering reward over-optimization in llm with demonstration-guided reinforcement  
750 learning. *arXiv preprint arXiv:2404.19409*, 2024.
- 751  
752 Giacomo Rizzolatti and Laila Craighero. The mirror-neuron system. *Annu. Rev. Neurosci.*, 27(1):  
753 169–192, 2004.
- 754  
755 Stéphane Ross, Geoffrey Gordon, and Drew Bagnell. A reduction of imitation learning and struc-  
756 tured prediction to no-regret online learning. In *Proceedings of the fourteenth international con-*  
757 *ference on artificial intelligence and statistics*, pp. 627–635. JMLR Workshop and Conference  
758 Proceedings, 2011.
- 759  
760 Stefan Schaal. Is imitation learning the route to humanoid robots? *Trends in cognitive sciences*, 3  
761 (6):233–242, 1999.

- 756 Yu-Zhe Shi, Haofei Hou, Zhangqian Bi, Fanxu Meng, Xiang Wei, Lecheng Ruan, and Qining Wang.  
757 Autodsl: Automated domain-specific language design for structural representation of procedures  
758 with constraints. *arXiv preprint arXiv:2406.12324*, 2024.
- 759 Noah Shinn, Federico Cassano, Edward Berman, Ashwin Gopinath, Karthik Narasimhan, and  
760 Shunyu Yao. Reflexion: Language agents with verbal reinforcement learning. In *Neural In-*  
761 *formation Processing Systems*, 2023.
- 762 Ishika Singh, Valts Blukis, Arsalan Mousavian, Ankit Goyal, Danfei Xu, Jonathan Tremblay, Dieter  
763 Fox, Jesse Thomason, and Animesh Garg. Progprompt: Generating situated robot task plans using  
764 large language models. In *2023 IEEE International Conference on Robotics and Automation*  
765 *(ICRA)*, pp. 11523–11530. IEEE, 2023.
- 766 Chan Hee Song, Jiaman Wu, Clayton Washington, Brian M. Sadler, Wei-Lun Chao, and Yu Su.  
767 Llm-planner: Few-shot grounded planning for embodied agents with large language models. In  
768 *IEEE/CVF International Conference on Computer Vision (ICCV)*, 2023.
- 769 Hao Sun and Mihaela van der Schaar. Inverse-rllignment: Inverse reinforcement learning from  
770 demonstrations for llm alignment. *arXiv preprint arXiv:2405.15624*, 2024.
- 771 Mirac Suzgun, Nathan Scales, Nathanael Schärli, Sebastian Gehrmann, Yi Tay, Hyung Won Chung,  
772 Aakanksha Chowdhery, Quoc V Le, Ed H Chi, Denny Zhou, et al. Challenging big-bench tasks  
773 and whether chain-of-thought can solve them. *arXiv preprint arXiv:2210.09261*, 2022.
- 774 Bowen Tan, Yun Zhu, Lijuan Liu, Hongyi Wang, Yonghao Zhuang, Jindong Chen, Eric Xing, and  
775 Zhiting Hu. Redcoast: A lightweight tool to automate distributed training of llms on any gpu/tpus.  
776 *arXiv preprint arXiv:2310.16355*, 2023.
- 777 Bowen Tan, Yun Zhu, Lijuan Liu, Eric Xing, Zhiting Hu, and Jindong Chen. Cappy: Outperforming  
778 and boosting large multi-task llms with a small scorer. *Advances in Neural Information Processing*  
779 *Systems*, 36, 2024.
- 780 Hugo Touvron, Louis Martin, Kevin Stone, Peter Albert, Amjad Almahairi, Yasmine Babaei, Niko-  
781 lay Bashlykov, Soumya Batra, Prajjwal Bhargava, Shruti Bhosale, et al. Llama 2: Open founda-  
782 tion and fine-tuned chat models. *arXiv preprint arXiv:2307.09288*, 2023.
- 783 Sai Vemprala, Rogerio Bonatti, Arthur Bucker, and Ashish Kapoor. Chatgpt for robotics: Design  
784 principles and model abilities. *Microsoft Auton. Syst. Robot. Res*, 2:20, 2023.
- 785 Lirui Wang, Yiyang Ling, Zhecheng Yuan, Mohit Shridhar, Chen Bao, Yuzhe Qin, Bailin Wang,  
786 Huazhe Xu, and Xiaolong Wang. Gensim: Generating robotic simulation tasks via large language  
787 models. *CoRR*, abs/2310.01361, 2023a.
- 788 Ruoyao Wang, Peter Jansen, Marc-Alexandre Côté, and Prithviraj Ammanabrolu. Scienceworld:  
789 Is your agent smarter than a 5th grader? In *Proceedings of the 2022 Conference on Empirical*  
790 *Methods in Natural Language Processing*, pp. 11279–11298, 2022.
- 791 Yufei Wang, Zhou Xian, Feng Chen, Tsun-Hsuan Wang, Yian Wang, Zackory Erickson, David Held,  
792 and Chuang Gan. Robogen: Towards unleashing infinite data for automated robot learning via  
793 generative simulation. *CoRR*, abs/2311.01455, 2023b.
- 794 Zihao Wang, Shaofei Cai, Guanzhou Chen, Anji Liu, Xiaojuan Ma, and Yitao Liang. Describe,  
795 explain, plan and select: Interactive planning with large language models enables open-world  
796 multi-task agents. *arXiv preprint arXiv:2302.01560*, 2023c.
- 797 Jason Wei, Xuezhi Wang, Dale Schuurmans, Maarten Bosma, brian ichter, Fei Xia, Ed H. Chi,  
798 Quoc V Le, and Denny Zhou. Chain of thought prompting elicits reasoning in large language  
799 models. In *Advances in Neural Information Processing Systems*, 2022.
- 800 Zhenyu Wu, Ziwei Wang, Xiuwei Xu, Jiwen Lu, and Haibin Yan. Embodied task planning with  
801 large language models. *arXiv preprint arXiv:2307.01848*, 2023.

- 810 Tianbao Xie, Siheng Zhao, Chen Henry Wu, Yitao Liu, Qian Luo, Victor Zhong, Yanchao Yang, and  
811 Tao Yu. Text2reward: Automated dense reward function generation for reinforcement learning.  
812 *CoRR*, abs/2309.11489, 2023.  
813
- 814 Weimin Xiong, Yifan Song, Xiutian Zhao, Wenhao Wu, Xun Wang, Ke Wang, Cheng Li, Wei Peng,  
815 and Sujian Li. Watch every step! Llm agent learning via iterative step-level process refinement.  
816 *arXiv preprint arXiv:2406.11176*, 2024.
- 817 Haoran Xu, Xianyuan Zhan, Honglei Yin, and Huiling Qin. Discriminator-weighted offline imitation  
818 learning from suboptimal demonstrations. In *Proceedings of the 39th International Conference on*  
819 *Machine Learning*, pp. 24725–24742, 2022. URL [https://proceedings.mlr.press/  
820 v162/xu221.html](https://proceedings.mlr.press/v162/xu221.html).
- 821 Chengrun Yang, Xuezhi Wang, Yifeng Lu, Hanxiao Liu, Quoc V Le, Denny Zhou, and Xinyun Chen.  
822 Large language models as optimizers. In *International Conference on Learning Representations*,  
823 2024.  
824
- 825 Shunyu Yao, Dian Yu, Jeffrey Zhao, Izhak Shafran, Thomas L. Griffiths, Yuan Cao, and Karthik R  
826 Narasimhan. Tree of thoughts: Deliberate problem solving with large language models. In *Neural*  
827 *Information Processing Systems*, 2023a.
- 828 Shunyu Yao, Jeffrey Zhao, Dian Yu, Nan Du, Izhak Shafran, Karthik R Narasimhan, and Yuan Cao.  
829 React: Synergizing reasoning and acting in language models. In *International Conference on*  
830 *Learning Representations*, 2023b.  
831
- 832 Weiran Yao, Shelby Heinecke, Juan Carlos Niebles, Zhiwei Liu, Yihao Feng, Le Xue, Rithesh R N,  
833 Zeyuan Chen, Jianguo Zhang, Devansh Arpit, Ran Xu, Phil L Mui, Huan Wang, Caiming Xiong,  
834 and Silvio Savarese. Retroformer: Retrospective large language agents with policy gradient op-  
835 timization. In *The Twelfth International Conference on Learning Representations*, 2024. URL  
836 <https://openreview.net/forum?id=KOZu91CzbK>.
- 837 Wenhao Yu, Nimrod Gileadi, Chuyuan Fu, Sean Kirmani, Kuang-Huei Lee, Montse Gonzalez Aren-  
838 nas, Hao-Tien Lewis Chiang, Tom Erez, Leonard Hasenclever, Jan Humplik, Brian Ichter, Ted  
839 Xiao, Peng Xu, Andy Zeng, Tingnan Zhang, Nicolas Heess, Dorsa Sadigh, Jie Tan, Yuval Tassa,  
840 and Fei Xia. Language to rewards for robotic skill synthesis. *CoRR*, abs/2306.08647, 2023.
- 841 Yuexiang Zhai, Hao Bai, Zipeng Lin, Jiayi Pan, Shengbang Tong, Yifei Zhou, Alane Suhr, Sain-  
842 ing Xie, Yann LeCun, Yi Ma, and Sergey Levine. Fine-tuning large vision-language models as  
843 decision-making agents via reinforcement learning, 2024. URL [https://arxiv.org/abs/  
844 2405.10292](https://arxiv.org/abs/2405.10292).
- 845 Dan Zhang, Sining Zhou, Yisong Yue, Yuxiao Dong, and Jie Tang. Rest-mcts\*: Llm self-  
846 training via process reward guided tree search. *arXiv preprint arXiv:2406.03816*, 2024.  
847
- 848 Wayne Xin Zhao, Kun Zhou, Junyi Li, Tianyi Tang, Xiaolei Wang, Yupeng Hou, Yingqian Min,  
849 Beichen Zhang, Junjie Zhang, Zican Dong, et al. A survey of large language models. *arXiv*  
850 *preprint arXiv:2303.18223*, 2023a.
- 851 Zirui Zhao, Wee Sun Lee, and David Hsu. Large language models as commonsense knowledge for  
852 large-scale task planning. *Advances in Neural Information Processing Systems*, 36, 2023b.  
853
- 854 Andy Zhou, Kai Yan, Michal Shlapentokh-Rothman, Haohan Wang, and Yu-Xiong Wang. Lan-  
855 guage agent tree search unifies reasoning acting and planning in language models. *arXiv preprint*  
856 *arXiv:2310.04406*, 2023a.
- 857 Zhehua Zhou, Jiayang Song, Kunpeng Yao, Zhan Shu, and Lei Ma. Isr-llm: Iterative self-  
858 refined large language model for long-horizon sequential task planning. *arXiv preprint*  
859 *arXiv:2308.13724*, 2023b.  
860  
861  
862  
863



## 864 A THEORETICAL PROOF

### 865 A.1 PROOF OF LEMMA 3.1

866 *Proof.* We recall the critic-regularized problem as follows.

$$867 \mathcal{L}^{\text{dgap}} = \mathbb{E}_{s \sim d_{\text{llm}}^{\pi}, a \sim \pi^{\text{llm}}} [R_{\phi}(s, a)] - \beta D_{\text{KL}}[\pi_{\theta}(a|s) \| \pi^{\text{llm}}(a|s)]. \quad \text{s.t.} \int_a \pi_{\theta}(a|s) da = 1. \quad (7)$$

872 In a constrained optimization problem,  $\beta$  can be considered as a Lagrange multiplier that controls  
873 the KL-divergence between the learned policy and the basic LLM policy. Then we convert it into a  
874 Lagrangian form by introducing a factor  $\alpha_s$  as

$$875 \mathcal{L}(\pi_{\theta}, \beta, \alpha) = \int_s d_{\text{llm}}^{\pi}(s) \int_a \pi^{\text{llm}}(a|s) R_{\phi}(s, a) dad s - \beta \int_s d_{\text{llm}}^{\pi}(s) D_{\text{KL}}[\pi_{\theta}(\cdot|s) \| \pi^{\text{llm}}(\cdot|s)] ds \\ 876 + \int_s \alpha_s \left( 1 - \int_a \pi(a|s) da \right) ds, \quad (8)$$

881 with  $\beta$  and  $\alpha = \{\alpha_s | \forall s \in \mathcal{S}\}$  corresponding to the Lagrange multipliers. Differentiating  $\mathcal{L}(\pi_{\theta}, \beta, \alpha)$   
882 with respect to  $\pi(a|s)$  results in

$$883 \frac{\partial \mathcal{L}}{\partial \pi(a|s)} = d_{\text{llm}}^{\pi}(s) R_{\phi}(s, a) - \beta d_{\text{llm}}^{\pi}(s) \log \pi_{\theta}(a|s) + \beta d_{\text{llm}}^{\pi}(s) \log \pi^{\text{llm}}(a|s) - \beta d_{\text{llm}}^{\pi}(s) - \alpha_s. \quad (9)$$

886 Setting to zero and solving for  $\pi_{\theta}(a|s)$  gives

$$887 \log \pi_{\theta} = \frac{1}{\beta} R_{\phi}(s, a) + \log \pi^{\text{llm}}(a|s) - 1 - \frac{\alpha_s}{\beta \cdot d_{\text{llm}}^{\pi}}. \quad (10)$$

890 Then we have

$$891 \pi_{\theta}(a|s) = \pi^{\text{llm}}(a|s) \exp\left(\frac{1}{\beta} R_{\phi}(s, a)\right) \exp\left(-\frac{\alpha_s}{\beta} \frac{1}{d_{\text{llm}}^{\pi}} - 1\right). \quad (11)$$

894 Since  $\int_a \pi(a|s) = 1$ , the second exponential term is the partition function  $Z(s)$  that normalizes the  
895 conditional action distribution, as

$$896 Z(s) = \exp\left(\frac{\alpha_s}{\beta} \frac{1}{d_{\text{llm}}^{\pi}} + 1\right) = \int_{a'} \pi^{\text{llm}}(a'|s) \exp\left(\frac{1}{\beta} R_{\phi}(s, a')\right) da'. \quad (12)$$

900 Then the optimal policy is given by

$$901 \pi_{\theta}^*(a|s) = \frac{1}{Z(s)} \pi^{\text{llm}}(a|s) \exp\left(\frac{1}{\beta} R_{\phi}(s, a)\right), \quad (13)$$

904 which concludes our proof.  $\square$

### 906 A.2 PROOF OF COROLLARY 3.2

908 *Proof.* We remark that the objective function  $\mathcal{L}^{\text{dgap}}$  can also be formulated as a constrained opti-  
909 mization problem. Considering a tabular case with finite state and actions, we have

$$910 \pi_{\theta}^* = \arg \max_{\pi_{\theta}} \mathbb{E}_{s \sim d_{\text{llm}}^{\pi}} \left[ \sum_a \pi^{\text{llm}}(s, a) Q^{\pi^{\text{llm}}}(s, a) \right] \quad \text{s.t.} \quad D_{\text{KL}}[\pi_{\theta}(\cdot|s) \| \pi^{\text{llm}}(\cdot|s)] \leq \epsilon, \forall s, \quad (14)$$

913 where we use  $Q^{\pi}(s, a)$  to denote  $\mathbb{E}_{\pi}[R_{\phi}(s, a)]$ . It is easy to check that equation 14 has the same  
914 solution as equation 7 by relaxing the hard KL constraint into a soft constraint with a coefficient  $\beta$ .  
915 From equation 14, we have

$$916 \sum_a \pi_{\theta}^*(s, a) Q^{\pi^{\text{llm}}}(s, a) \geq \sum_a \pi^{\text{llm}}(s, a) Q^{\pi^{\text{llm}}}(s, a), \forall s. \quad (15)$$

Then we have

$$\begin{aligned}
 Q^{\pi^{\text{llm}}}(s, a) &= \mathbb{E} \left[ r(s_t, a_t) + \sum \pi^{\text{llm}}(a_{t+1}|s_{t+1}) Q^{\pi^{\text{llm}}}(s_{t+1}, a_{t+1}) \middle| s_t = s, a_t = a \right] \\
 &\leq \mathbb{E} \left[ r(s_t, a_t) + \sum \pi_{\theta}^*(a_{t+1}|s_{t+1}) Q^{\pi^{\text{llm}}}(s_{t+1}, a_{t+1}) \middle| s_t = s, a_t = a \right] \\
 &= \mathbb{E} \left[ r(s_t, a_t) + \sum \pi_{\theta}^*(a_{t+1}|s_{t+1}) \left[ r(s_{t+1}, a_{t+1}) + \sum \pi^{\text{llm}}(a_{t+2}|s_{t+2}) Q^{\pi^{\text{llm}}}(s_{t+2}, a_{t+2}) \right] \middle| \dots \right] \\
 &\leq \mathbb{E} \left[ r(s_t, a_t) + \sum \pi_{\theta}^*(a_{t+1}|s_{t+1}) \left[ r(s_{t+1}, a_{t+1}) + \sum \pi_{\theta}^*(a_{t+2}|s_{t+2}) Q^{\pi^{\text{llm}}}(s_{t+2}, a_{t+2}) \right] \middle| \dots \right].
 \end{aligned} \tag{16}$$

Repeat this process to expand the equation, we have

$$Q^{\pi^{\text{llm}}}(s, a) \leq \mathbb{E}_{\pi_{\theta}^*} \left[ \sum_{k=0}^{T-t-1} \gamma^k r(s_{t+k}, s_{t+k}) \middle| s_t = s, a_t = a \right] = Q^{\pi_{\theta}^*}(s, a), \tag{17}$$

which concludes our proof.  $\square$

## B LM FINE-TUNING

We selected FLAN-T5-large as the base model due to its fine-tuning on datasets phrased as instructions, which improves its ability to follow and respond to instructions. According to the research detailed in (Chung et al., 2024), the model architecture includes:

- Number of layers: 24
- Number of attention heads: 16
- Hidden layer size: 1024
- Feedforward Network Size: 4096
- Activation Function: ReLU (Rectified Linear Unit)
- Total parameters: 770 million

Further we conduct imitation learning on FLAN-T5-Large using expert data in format of  $(l, h_t) \rightarrow a_{\pi^{\text{oracle}}(l, s_t)}$ . The data primarily encompasses three components: 1.a description of the task, 2.a record of historical actions, and 3.the actions that ought to be executed.The specifics are delineated below.

### ScienceWorld:

```

{"input": "Your task is to measure the melting point of lead, which is located around the kitchen. 10. look around.", "Action": "go to hallway"}
{"input": "Your task is to measure the melting point of lead, which is located around the kitchen. 10. look around. 9. go to hallway.", "Action": "open door to kitchen"}
{"input": "Your task is to measure the melting point of lead, which is located around the kitchen. 10. look around. 9. go to hallway. 8. open door to kitchen.", "Action": "go to kitchen"}

```

### VirtualHome:

```

{"input": "Task: Pay bills. [Walk] <home_office> (1)", "Action": "[Walk] <filing_cabinet> (1)"}
{"input": "Task: Pay bills. [Walk] <home_office> (1), [Walk] <filing_cabinet> (1)", "Action": "[Find] <bills> (1)"}
{"input": "Task: Pay bills. [Walk] <home_office> (1), [Walk] <filing_cabinet> (1), [Find] <bills> (1)", "Action": "[Grab] <bills> (1)"}

```

Then we refined FLAN-T5-large with the dataset as previously outlined, including 15k samples from ScienceWorld and 34k from VirtualHome. For the training, we employed the Adam optimizer with an epsilon value of 1e-06, a learning rate of 1e-4, and a batch size of 32. We conducted 3 training epochs comprising 25000 steps in total. We employ four A100 GPUs for conducting this task, consuming eight hours.

## C DISCRIMINATOR TRAINING

**Data Preparation** For training the discriminator, we collected a diverse dataset consisting of positive, negative and augmented samples, as illustrated in 3.1. Our motivation to assess the generalization necessitated the judicious use of expert data, thus preventing its overuse, particularly for tasks like *Measuring Boiling Point*, *Testing Conductivity*, and *Growing*, each initially comprising approximately 10k samples. Thus in ScienceWorld, to mitigate the dependency on expert information, we reduced the expert samples for each task to 1.5k, resulting in a total expert dataset of 45k. In parallel, we sampled 45k negative random samples. Finally, we generated 400k augmented samples, thereby creating a comprehensive pool of 500k samples. In VirtualHome, we utilized the entirety of available expert samples, given the infrequency of task repetition and a total count of only 34k. We constructed a dataset of 400k instances in a manner similar to that employed for ScienceWorld. The specific format of the data is  $(l, h_t, a_t) \rightarrow q$ , represented as follows:

### ScienceWorld-Expert:

```
{"input": "Your task is to measure the melting point of lead, which is located around the kitchen. 10. look around. Action: go to hallway", "Score": "10" }
```

```
{"input": "Your task is to measure the melting point of lead, which is located around the kitchen. 10. look around. 9. go to hallway. Action: open door to kitchen", "Score": "10" }
```

### ScienceWorld-Random:

```
{"input": "Your task is to measure the melting point of lead, which is located around the kitchen. 10. look around. Action: look at art studio", "Score": "0" }
```

```
{"input": "Your task is to measure the melting point of lead, which is located around the kitchen. 10. look around. 9. go to hallway. Action: put down orange", "Score": "0" }
```

### ScienceWorld-Augmented:

```
{"input": "Your task is to measure the melting point of lead, which is located around the kitchen. 10. look around. Action: look at hallway", "Score": "9.03" }
```

```
{"input": "Your task is to measure the melting point of lead, which is located around the kitchen. 10. look around. 9. look at hallway. Action: open door to outside", "Score": "6.13" }
```

```
{"input": "Your task is to measure the melting point of lead, which is located around the kitchen. 10. look around. 9. look at hallway. 8. open door to outside. Action: teleport to kitchen", "Score": "8.87" }
```

....

### VirtualHome-Expert:

```
{"input": "Task: Pay bills. [Walk] <home_office> (1). Action: [Walk] <filing_cabinet> (1)", "Score": "10" }
```

```
{"input": "Task: Pay bills. [Walk] <home_office> (1), [Walk] <filing_cabinet> (1). Action: [Find] <bills> (1)", "Score": "10" }
```

### VirtualHome-Random:

```
{"input": "Task: Pay bills. [Walk] <home_office> (1). Action: [open] <microwave> (1)", "Score": "0" }
```

```
{"input": "Task: Pay bills. [Walk] <home_office> (1), [Walk] <filing_cabinet> (1). Action: [grab] <chicken> (1)", "Score": "0" }
```

### VirtualHome-Augmented:

```
{"input": "Task: Pay bills. [Walk] <home_office> (1). Action: [walk] <kitchencabinet> (1)", "Score": "8.32" }
```

```
{"input": "Task: Pay bills. [Walk] <home_office> (1), [walk] <kitchencabinet> (1). Action: [grab] <bills> (1)", "Score": "7.42" }
```

```
{"input": "Task: Pay bills. [Walk] <home_office> (1), [walk] <kitchencabinet> (1), [grab] <bills> (1). Action: [walk] <livingroom>(1)", "Score": "6.99" }
```

.....

$$Q = \begin{cases} 10 & \text{if data in } \mathcal{B}_e \\ 0 & \text{if data in } \mathcal{B}_r \\ \text{Sim}(a_{\pi^{\text{bc}}}, a_{\pi^{\text{oracle}}}) * 10 & \text{if data in } \mathcal{B}_a \end{cases} \quad (18)$$

**Model Architecture** We employ RoBERTa complemented by a linear head, which facilitates direct output for regression tasks. This configuration leverages RoBERTa’s robust contextual embedding capabilities while the linear head(768,1) simplifies the mapping from embedded space to target labels, the model architecture is listed:

- Number of Layers: 12 layers
- Hidden Size: 768
- Number of Attention Heads: 12
- Feedforward Network Size: 3072
- Activation Function: GELU
- Total parameters: 125 million

**Training Procedure** We assembled datasets containing 500k instances for ScienceWorld and 400k instances for VirtualHome separately, each formatted as (instruction, action, score). The model was initialized with RoBERTa parameters and optimized using the AdamW optimizer a learning rate of  $1e-5$ , a warmup rate of 0.1, and a batch size of 32. For detailed training specifications, please refer to (Tan et al., 2023). During training, the inputs comprising instructions and actions are given into the RoBERTa model to obtain the last hidden state. This state is then processed through a linear head to compute scores, which are compared against labels to determine the L2 loss. Subsequently, this loss is used to update the model parameters. We employ four A100 GPUs for conducting this task, consuming around forty hours.

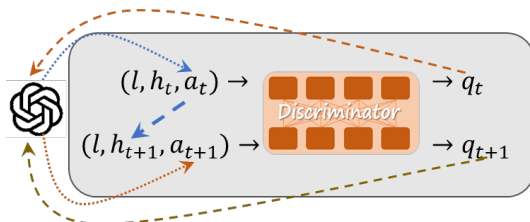


Figure 6: Illustration of applying discriminator to LLM

**Discriminator Application** Fig. 6 depicts the functioning of a discriminator within a LLM interacting framework. Initially, the discriminator receives input tuples composed of a task description  $l$ , history actions  $h_t$ , and response action of LLM  $a_t$ . It evaluates these inputs to generate a score  $q_t$ , which assesses the relevance to the expert response of the input tuple.

As the interaction progresses, the discriminator’s inputs are advanced to the subsequent state, encapsulated by the tuple  $(l, h_{t+1}, a_{t+1})$ . Here,  $h_{t+1}$  incorporates the previously generated action  $a_t$  and based on the new context the LLM subsequently derives the new action  $a_{t+1}$ . In response, the discriminator calculates a subsequent score,  $q_{t+1}$ , for this new input.

The blue and orange dashed lines in the diagram represent information transmission at different time steps, highlighting the iterative and conditional role of the discriminator in evaluating successive actions in the sequence.

Actions generated by the Large Language Model (LLM) are not executed immediately but instead stored in an action buffer. These actions are subsequently scored by a discriminator prior to execution. If the score is below 4, a replanning process called Score-based Search is triggered, wherein the discriminator evaluates and selects the highest-scoring action from the set of valid actions for execution, as shown in Fig. 7. Conversely, if the score exceeds 8, the action is highlighted in the subsequent interaction round by including it as ‘Noted: history action-score pair’ in the prompt, ensuring its prominence. This procedure ensures that the discriminator not only accesses LLM inferences but also grounds actions when necessary to prevent anomalies.

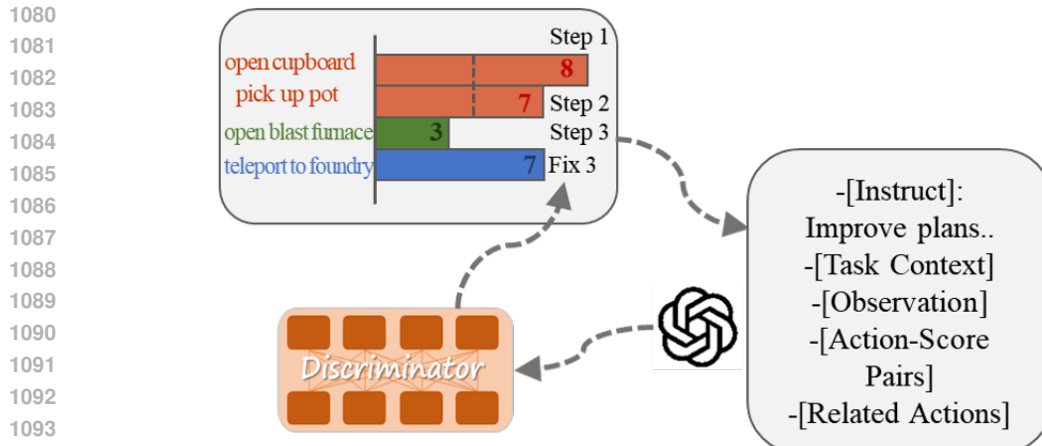


Figure 7: Illustration of score-based search

## D STATISTICS AND DETAILS IN PLANNING

### D.1 EXPERIMENT STATICS

Table 3 provides an overview of the 30 distinct tasks within the ScienceWorld benchmark, categorized by task type, topic, and associated attributes. For the evaluation phase, we optimized time efficiency by selecting only the first 10 variations for tasks that originally had more than 10 test variations, resulting in a total of 270 task variations. This approach ensured fair and cost-effective comparisons across agents. Table 3 also includes trajectory statistics, where \*Len represents the average length of the oracle agent’s trajectories, offering insight into task complexity across different task types.

### D.2 BASELINES

**ScienceWorld Baselines** We benchmark DGAP methodology against three kinds of approaches: **(i) Behavior Cloning-Only:** The Text Decision Transformer (TDT) leverages behavior cloning and incorporates reward-to-go as an input, which enables the model to predict actions designed to maximize future expected rewards (Chen et al., 2021). **(ii) Planning via Self-Reflection:** Techniques such as ReAct (Yao et al., 2023b) and Reflexion (Shinn et al., 2023) integrate a self-reasoning mechanism within the planning process to enhance reasoning capabilities. **(iii) Demonstration-Driven Method:** SwiftSage (Lin et al., 2023) amalgamates rapid thinking with demonstrations as our method and methodical reasoning, establishing itself as the state-of-the-art baseline in ScienceWorld, making it our primary focus of compare. For our implementations, we utilize Llama3-70B and GPT-4 as the foundational Large Language Models. Specifically, **S-GPT4** represents the SwiftSage method utilizing GPT-4, while **D-GPT4** denotes the DGAP strategy integrated with GPT-4. Similarly, **S-Llama3** corresponds to the SwiftSage approach adapted Llama3-70B, and **D-Llama3** signifies the DGAP method deployed with Llama3-70B. TDT ReAct and Reflexion utilize GPT-4.

**VirtualHome Baselines** We evaluate DGAP against three kinds of approaches: **(i) Planning based:** LLMs employ a method that directly generates planning results through in-context learning, such as ProgPrompt (Singh et al., 2023). **(ii) Reasoning based:** In this approach, LLMs are rendered with a specialized prompting mechanism to enhance their inference when tackling complex tasks, such as Inner Monologue (Huang et al., 2022b). **(iii) Search based:** This approach reframes the inference process into plan sampling and tree construction, thereby establishing a comprehensive and efficient pathway for task execution (Hu et al., 2023).

1134  
1135  
1136  
1137  
1138  
1139  
1140  
1141  
1142  
1143  
1144  
1145  
1146  
1147  
1148  
1149  
1150  
1151  
1152  
1153  
1154  
1155  
1156  
1157  
1158  
1159  
1160  
1161  
1162  
1163  
1164  
1165  
1166  
1167  
1168  
1169  
1170  
1171  
1172  
1173  
1174  
1175  
1176  
1177  
1178  
1179  
1180  
1181  
1182  
1183  
1184  
1185  
1186  
1187

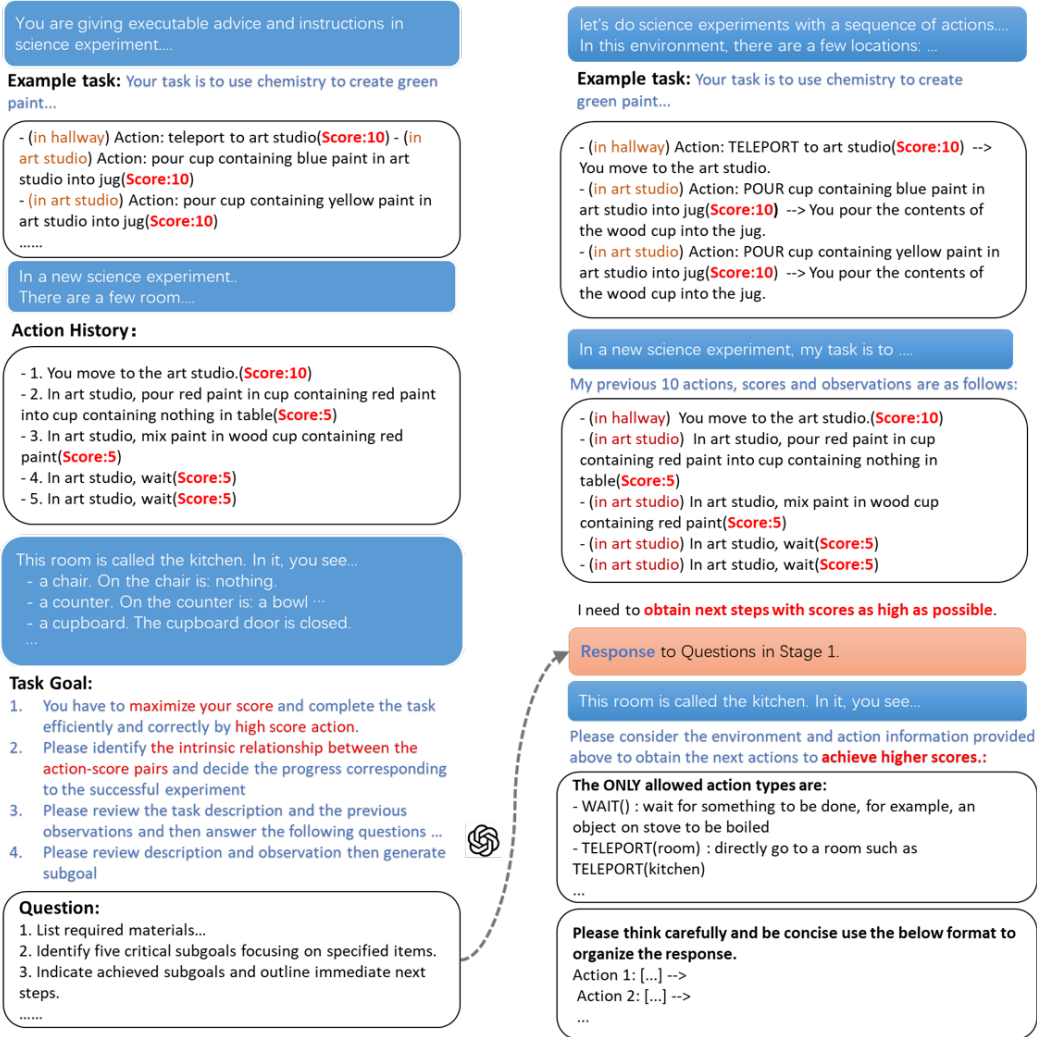


Figure 8: Prompt Template in ScienceWorld

Task Num	Type	Topic	Name	*Lens
1	1-1	Matter	Changes of State (Boiling)	107.7
2	1-4	Matter	Changes of State (Any)	75.2
3	6-1	Chemistry	Mixing (generic)	33.6
4	6-2	Chemistry	Mixing paints (secondary colours)	15.1
5	6-3	Chemistry	Mixing paints (tertiary colours)	23
6	4-4	Classification	Find an animal	14.6
7	4-1	Classification	Find a living thing	14.6
8	4-2	Classification	Find a non-living thing	8.8
9	4-3	Classification	Find a plant	12.6
10	1-3	Matter	Changes of State (Freezing)	88.9
11	5-2	Biology	Grow a fruit	79.6
12	5-1	Biology	Grow a plant	69.5
13	8-2	Biology	Identify life stages (animal)	16.3
14	8-1	Biology	Identify life stages (plant)	40
15	9-1	Forces	Inclined Planes (determine angle)	97
16	9-2	Forces	Friction (known surfaces)	84.9
17	9-3	Forces	Friction (unknown surfaces)	123.1
18	7-1	Biology	Identify longest-lived animal	7
19	7-3	Biology	Identify longest-lived animal	8
20	7-2	Biology	Identify shortest-lived animal	7
21	2-2	Measurement	Measuring Boiling Point (known)	35.2
22	2-3	Measurement	Measuring Boiling Point (unknown)	65
23	1-2	Matter	Changes of State (Melting)	78.6
24	10-1	Biology	Mendelian Genetics (known plants)	130.1
25	10-2	Biology	Mendelian Genetics (unknown plants)	132.1
26	3-1	Electricity	Create a circuit	13.6
27	3-2	Electricity	Renewable vs Non-renewable Energy	20.8
28	3-3	Electricity	Test Conductivity (known)	25.6
29	3-4	Electricity	Test Conductivity (unknown)	29
30	2-1	Measurement	Use Thermometer	21.4
Short ( $0 < *Len \leq 20$ )			Total: 10	11.76
Medium ( $20 < *Len \leq 50$ )			Total: 8	28.58
Long ( $*Len > 50$ )			Total: 12	94.30
<b>Overall</b>			Total: 30	49.26

Table 3: The table presents detailed information on the 30 distinct tasks in the ScienceWorld benchmark, categorized by task number, type, topic, and name. \*Len refers to the average length of the oracle agent’s trajectories, based on which tasks are grouped into short, medium, and long categories, indicating the complexity and duration of each task. Additionally, the breakdown by task type (e.g., Matter, Biology, Chemistry) highlights the diversity of domains covered in the benchmark.

### D.3 PROMPT DETAILS

Our prompt design was inspired by the two-stage framework of SwiftSage (Lin et al., 2023), and further incorporate DGAP information at various places in the context(marked in red).

Our prompt was influenced by ProgPrompt (Singh et al., 2023) and Tree-Planner (Hu et al., 2023), and incorporates score-related information into the context(marked in red).

## E ADDITIONAL RESULTS AND ANALYSIS

**Ablation Study** In **ScienceWorld**, the tasks 1-15 are based on the DGAP-Llama3, whereas tasks 16-30 are according to DGAP-GPT4, both excluding content related to scores from the context

1242  
 1243  
 1244 from actions import walk <obj>, grab <obj>, switchon  
 1245 <obj>, switchoff <obj>...  
 1246 The total task goal: put\_chicken\_on kitchentable(id:123)#  
 1247 The completed task goal:  
 1248  
 1249  
 1250 Rule:  
 1251 # remeber if the key object INSIDE kitchencabinet...  
 1252  
 1253 The completed Action:  
 1254 [walk] <livingroom> (262) (Score:8)  
 1255 [walk] <pancake> (342) (Score:8)  
 1256 [grab] <pancake> (342) (Score:9)  
 1257 .....  
 1258  
 1259 There are some examples:  
 1260 The task goal: put one cupcake in stove and switch on  
 1261 stove  
 1262 find('kitchencabinet(id:131)') (Score:10)  
 1263 open('kitchencabinet(id:131)') (Score:10)  
 1264 find('cupcake(id:334)') (Score:10)  
 1265 grab('cupcake(id:334)') (Score:10)  
 1266 .....  
 1267  
 1268 Question:  
 1269 #The currnet task goal: find\_stove(id:150):  
 1270 #Remember **obtain actions with scores as high as possible**  
 1271 Def task():.....

Figure 9: Prompt Template in VirtualHome

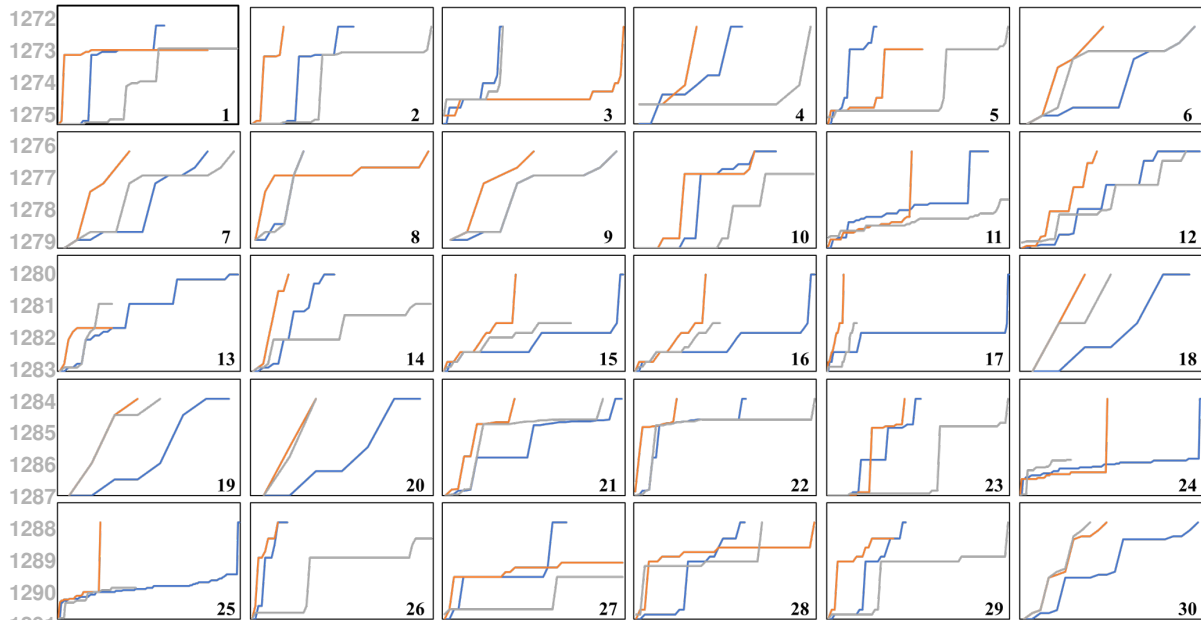


Figure 10: Visualizing trajectories of **DGAP**, **SWIFTSAGE** and **ORACLE**, the x-axis represents time steps, ranging from 0 to  $T$ , while the y-axis denotes scores, which vary from 0 to 100. Each graph illustrates the trajectories corresponding to different tasks in test variation. Task identifiers are positioned at the bottom right of each figure, whose detailed information can be found in Tab. 3



1296  
1297  
1298  
1299  
1300  
1301  
1302  
1303  
1304  
1305  
1306  
1307  
1308  
1309  
1310  
1311

Task	D-Llama3	w/o Score	Task	D-GPT4	New Data
1	<b>82.67</b>	77.33	16	<b>83.33</b>	78.57
2	<b>90.66</b>	76.00	17	71.43	<b>85.71</b>
3	<b>78.67</b>	66.50	18	<b>100.00</b>	100.00
4	<b>100.00</b>	100.00	19	<b>92.71</b>	92.71
5	68.00	<b>100.00</b>	20	<b>85.71</b>	78.57
6	<b>100.00</b>	85.71	21	<b>80.17</b>	62.86
7	<b>100.00</b>	87.50	22	<b>88.33</b>	50.14
8	<b>100.00</b>	100.00	23	<b>92.75</b>	80.67
9	76.29	<b>88.14</b>	24	87.71	<b>100.00</b>
10	<b>82.67</b>	65.33	25	<b>78.00</b>	46.14
11	<b>57.33</b>	45.86	26	<b>91.50</b>	83.00
12	<b>78.00</b>	73.43	27	<b>58.00</b>	50.50
13	<b>45.00</b>	40.00	28	<b>78.57</b>	77.80
14	<b>100.00</b>	100.00	29	<b>88.14</b>	87.43
15	57.14	<b>71.43</b>	30	<b>100.00</b>	61.43

1312  
1313

Table 4: Ablation study of DGAP in ScienceWorld

1314  
1315  
1316  
1317  
1318  
1319  
1320  
1321

	In-Distribution		NovelScenes		NovelTasks	
	EXEC.	SR.	EXEC.	SR.	EXEC.	SR.
<b>ProgPrompt</b>	87.33 ± 2.02	82.33 ± 1.76	38.67 ± 1.45	32.33 ± 1.45	49.67 ± 3.18	49.00 ± 3.21
<b>Inner Monologue</b>	79.67 ± 3.38	79.33 ± 3.18	54.33 ± 1.76	53.33 ± 1.76	47.33 ± 1.67	46.00 ± 1.15
<b>Tree Planner</b>	-	-	<b>89.33 ± 0.17</b>	41.67 ± 3.20	<b>90.33 ± 0.32</b>	52.33 ± 2.03
<b>DGAP-Llama3</b>	90.67 ± 0.86	84.33 ± 2.12	63.00 ± 1.68	56.33 ± 1.12	78.33 ± 1.03	68.00 ± 2.03
<b>DGAP-GPT4</b>	<b>93.33 ± 1.76</b>	<b>88.00 ± 2.45</b>	71.67 ± 1.15	<b>62.67 ± 1.33</b>	73.67 ± 1.15	<b>72.17 ± 3.18</b>
<b>D-GPT4 w/o Score</b>	92.33 ± 2.19	86.00 ± 2.65	70.67 ± 2.67	60.67 ± 0.63	70.33 ± 3.06	70.00 ± 3.21

1322  
1323

Table 5: ABLATION STUDY OF DGAP AND BASELINES

1324  
1325  
1326  
1327  
1328  
1329  
1330

and scoring thresholds mechanism for handling the exception. The results reveal that tasks 5, 9, 15, 17, and 24 exhibited better performance after the removal of score-related content, spanning both short and long task types. This phenomena likely stems from a significant deviation between the augmented data used for training the discriminator and the actual data encountered in real-world interactions in these tasks. It is noteworthy that tasks 6-3, 4-3, 9-1, 9-3, and 10-1 exhibit no significant performance improvements when evaluated against the SwiftSage baseline.

1331  
1332  
1333  
1334  
1335

In **VirtualHome** environment, we selected DGAP-GPT4 for an ablation study due to its significantly superior performance compared to DGAP-Llama3. The results indicate that, following the removal of score-related context and the absence of scoring thresholds mechanism, both the success rate and the execution rate decreased by 1 to 2 percent. This demonstrates that DSAP is effective not only in science tasks but also in household tasks, where it provides substantial guidance.

1336  
1337

E.1 ALFRED EXPERIMENTS

1338  
1339  
1340  
1341  
1342  
1343  
1344  
1345  
1346  
1347  
1348

Methods	Seen		Unseen	
	SR	GC	SR	GC
LLMPlanner	0.121	0.267	0.162	0.402
LoTaBench	0.255	0.442	0.241	0.398
Prompter	<b>0.494</b>	<b>0.560</b>	0.423	0.537
DGAP-3.5Turbo	0.121	0.267	0.162	0.402
DGAP-4o	0.462	0.507	<b>0.441</b>	<b>0.545</b>
DGAP-4o-v	0.323	0.404	0.381	0.414
DGAP-InternVL2-8B	0.236	0.291	0.246	0.391

1349

Table 6: Performance comparison across methods on ALFRED seen and unseen tasks.

## Analysis of Methods and Results

Table 6 compares several methods on **Seen** and **Unseen** environments using **Success Rate (SR)** and **Goal Completion (GC)** metrics. **LLMPlanner** and **LoTaBench** rely only on LLMs and expert data for in-context learning. **Prompter** integrates semantic map information and combines low-level parsing with LLMs. **DGAP-3.5Turbo** uses `gpt-3.5-turbo-0125` as the backbone model. **DGAP-4o** is based on Azure’s GPT-4o model. **DGAP-4o-v** shares the same GPT-4o backbone but incorporates updated environmental maps during the planning phase. **DGAP-InternVL2-8B** shares the same settings as DGAP-4o-v, including updated environmental maps.

**DGAP-4o** only uses textual environment information and one-fifth of the expert data for discriminator’s training, yet achieves competitive results. In Seen environments, DGAP achieves strong performance (SR: 0.462, GC: 0.507), slightly behind Prompter. However, in Unseen environments, DGAP outperforms Prompter in GC (0.545 vs. 0.537), demonstrating better generalization. On the other hand, **DGAP-4o-v**, which incorporates RGB images into the planning process, shows a decline in performance. It’s likely attributed to two main factors: (1) the prompts and discriminator have not been fully optimized to utilize visual information. (2) the RGB images may introduce ambiguous or redundant information rather than render location information. These observations suggest that the integration of visual data requires more refined strategies to fully unlock its potential benefits.

**Weaknesses of DGAP:** Despite its strengths, there are two notable limitations that affect its performance in certain scenarios:

- Inconsistent Ground Truth:** The ground truth action sequences occasionally lack logical coherence or completeness. For example, in the "Turn on the bedroom lamp" task, the ground truth includes extraneous steps such as "Pick up CellPhone" before toggling the lamp. In the "Put a plate in a cabinet" task, additional steps like "Place plate in the fridge on the top shelf" are required. Task "Put a bowl with a pencil in it on the desk," where the ground truth includes an unnecessary intermediate step to "Put the bowl on the Shelf." There are various such cases which introduce noise and reduce alignment between the generated actions and expected outcomes for LLM planning.

- Ambiguity in Object Location:** For tasks involving similar objects, selecting one randomly among them can often suffice to meet the task’s objective. However, in scenarios requiring precise identification of specific storage locations (e.g., determining the correct cabinet where an object is stored), DGAP faces challenges due to the absence of explicit spatial or semantic distinctions in the textual input. This limitation impacts its ability to perform accurate object placement, leading to reduced performance on tasks that rely on spatial reasoning and clear differentiation between similar storage units. .

## E.2 VH-LONG-TASK

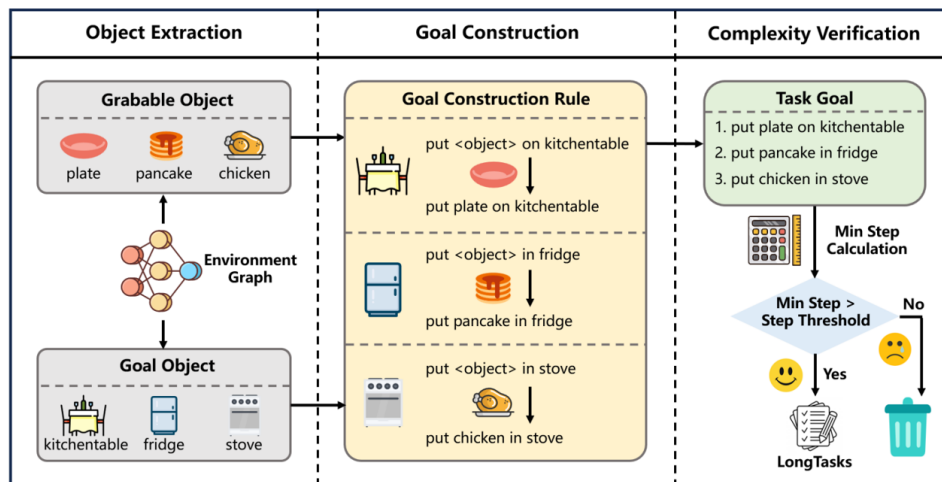


Figure 11: The framework of task constructing

**Extended Task Settings and Dataset Construction** To better reflect the high-dimensional and continuous tasks commonly encountered in real-world scenarios, which are typically multi-goal in nature, we extended the task settings in the VirtualHome environment to include **self-constructed long tasks**. By concatenating multiple task objectives, we created tasks exceeding **60 steps**, providing a more complex and realistic evaluation of long-horizon planning. The statistics of these extended tasks are summarized in the table below.

Dataset	Goals Number	Action Step	Objects Number	Objects Variety
In-Distribution	3.40	26.58	5.32	3.57
NovelScenes	3.39	26.27	5.32	3.56
NovelTasks	3.99	27.02	4.97	3.40
LongTasks	<b>9.74</b>	<b>77.01</b>	<b>15.79</b>	<b>8.50</b>

Table 7: Dataset statistics for various tasks in VirtualHome.

	Extreme-LONG		NovelScenes		NovelTasks	
	EXEC.	SR.	EXEC.	SR.	EXEC.	SR.
<b>ProgPrompt</b>	42.95 ± 1.22	16.03 ± 1.28	38.67 ± 1.45	32.33 ± 1.45	49.67 ± 3.18	49.00 ± 3.21
<b>Inner Monologue</b>	48.45 ± 1.05	16.16 ± 1.35	54.33 ± 1.76	53.33 ± 1.76	47.33 ± 1.67	46.00 ± 1.15
<b>Tree Planner</b>	<b>85.76 ± 1.40</b>	19.07 ± 1.79	<b>89.33 ± 0.17</b>	41.67 ± 3.20	<b>90.33 ± 0.32</b>	52.33 ± 2.03
<b>DGAP-GPT4o</b>	78.23 ± 1.15	<b>67.25 ± 2.10</b>	71.67 ± 1.15	<b>62.67 ± 1.33</b>	73.67 ± 1.15	<b>72.17 ± 3.18</b>

Table 8: OVERALL PERFORMANCE DGAP AND BASELINES ACROSS VH-LONG-TASK

Experimental results show that our method significantly outperforms the baseline in success rate, highlighting its superiority in handling high-complexity, long-horizon tasks and demonstrating the generalization capability of the discriminator.

### E.3 DISCRIMINATOR EVALUATION

Methods	Out-of-Distribution		In-Distribution		PER	OPer
	Acc	Var	Acc	Var		
4x	9.17	0.11	9.28	0.08	85.91	-
2x	9.16	0.11	9.28	0.08	85.91	-
0.4x	8.77	0.15	9.19	0.12	83.25	-
basis	8.08	0.36	8.16	0.36	82.26	83.53
basiswithforce	8.06	0.38	8.15	0.26	82.31	84.51
basiswithforcebio	8.91	0.20	9.01	0.17	84.98	86.68
1x(ours)	9.08	0.15	9.21	0.11	85.91	-

Table 9: Performance comparison of discriminator across data with different volumn and categories, with including PER and OPer metrics.

### E.4 SEARCH-BASED METHODS EVALUATION

We utilized the Vanna framework to construct the RAG pipeline, incorporating the **bge-large** model as the embedding backbone. The content matching process was based on a combination of task instructions and the initial environmental observations. We subsequently present its recall performance and evaluate its effectiveness within the context of SwiftSage’s deliberative reasoning, a highly effective in-context learning framework for ScienceWorld. The results are shown in Table 10

### E.5 QUALITATIVE ANALYSIS

**Feedback Mechanism** S-GPT4 failed in **Task8** due to its strict adherence to the rule prohibiting focus on counterparts when conditions are not fulfilled, exposing the limitations of relying solely

Task Type	*Len	S-GPT4	D-GPT4	Recall (%)	Performance
1-1(L)	107.70	97.04	<b>100.00</b>	91.8	90.89
1-2(L)	78.60	87.04	<b>92.75</b>	89.2	89.20
1-3(L)	88.90	72.78	<b>74.00</b>	87.2	57.20
1-4(L)	75.20	100.00	<b>100.00</b>	90.6	89.41
2-1(M)	21.40	99.17	<b>100.00</b>	94.8	93.99
2-2(M)	35.20	<b>88.17</b>	80.17	88.9	82.90
2-3(L)	65.00	<b>95.73</b>	88.33	86.4	86.40
3-1(S)	13.60	88.67	91.50	97.8	<b>100.00</b>
3-2(M)	20.80	55.33	<b>58.00</b>	89.6	49.60
3-3(M)	25.60	71.90	<b>78.57</b>	90.0	68.44
3-4(M)	29.00	77.86	88.14	91.5	<b>92.66</b>
4-1(S)	14.60	100.00	<b>100.00</b>	99.4	<b>100.00</b>
4-2(S)	8.80	100.00	<b>100.00</b>	98.2	<b>100.00</b>
4-3(S)	12.60	91.67	<b>100.00</b>	96.2	<b>100.00</b>
4-4(S)	14.60	100.00	<b>100.00</b>	98.5	<b>100.00</b>
5-1(L)	69.50	<b>74.59</b>	73.14	85.2	55.20
5-2(L)	79.60	<b>93.93</b>	90.57	90.8	61.58
6-1(M)	33.60	49.40	57.40	88.5	<b>58.50</b>
6-2(S)	15.10	100.00	<b>100.00</b>	98.5	<b>100.00</b>
6-3(M)	23.00	91.48	<b>92.43</b>	91.4	90.78
7-1(S)	7.00	95.00	<b>100.00</b>	97.1	<b>100.00</b>
7-2(S)	7.00	85.00	85.71	92.4	<b>93.63</b>
7-3(S)	8.00	<b>93.33</b>	92.71	95.8	<b>97.96</b>
8-1(M)	40.00	89.00	<b>100.00</b>	94.4	96.28
8-2(S)	16.30	<b>68.50</b>	38.50	93.3	<b>91.76</b>
9-1(L)	97.00	75.00	<b>75.00</b>	85.9	35.90
9-2(L)	84.90	70.00	<b>83.33</b>	86.1	69.10
9-3(L)	123.10	60.00	<b>71.43</b>	85.8	61.80
10-1(L)	130.10	<b>92.30</b>	87.71	92.4	82.74
10-2(L)	132.10	77.60	<b>78.00</b>	85.9	72.90
Short	11.76	<b>92.22</b>	90.84	97.3	98.12
Medium	28.58	77.79	<b>81.84</b>	90.5	79.14
Long	94.30	83.00	<b>84.52</b>	88.3	71.03
Overall	49.26	84.68	<b>85.91</b>	90.2	82.29

Table 10: Task performance comparison for S-GPT4, D-GPT4 with RAG

on the LLM, though the action is reasonable to some extent. In contrast, DGAP-GPT4 succeeded by leveraging discriminator feedback and re-planning through the LLM, which selected alternative yet equally reasonable actions to adaptively execute a comprehensive sequence. This included identifying, transporting, and arranging multiple items to fulfill all task requirements, emphasizing the importance of integrating robust feedback mechanisms and adaptive planning for complex, multi-step tasks, as shown in Figure 12.

**Enhanced Attention** The discriminator’s use of additional score labels enhances attention on relevant examples and prior actions, improving environmental interaction understanding and directly boosting planning quality without relying on re-planning. This is evident in **Task25**. As shown in Figure 13, where DGAP-generated actions are efficiently aligned with task objectives, focusing on the electric buzzer early and following a logical path to complete the circuit with minimal redundancy. In contrast, the other sequence exhibits inefficiencies, including unnecessary connections and delays, highlighting the limitations of planning without adequate score attention. This comparison underscores the discriminator’s role in enabling precise and efficient task execution.

1512  
1513  
1514  
1515  
1516  
1517  
1518  
1519  
1520  
1521  
1522  
1523  
1524  
1525  
1526  
1527  
1528  
1529  
1530  
1531  
1532  
1533  
1534  
1535  
1536  
1537  
1538  
1539  
1540  
1541  
1542  
1543  
1544  
1545  
1546  
1547  
1548  
1549  
1550  
1551  
1552  
1553  
1554  
1555  
1556  
1557  
1558  
1559  
1560  
1561  
1562  
1563  
1564  
1565

**Your task is to find a(n) plant. First, focus on the thing. Then, move it to the yellow box in the bedroom**



DGAP-GPT4

SwiftSage-GPT4

- 1. look around
  - 2. teleport to greenhouse
  - 3. focus on flower pot 1
- Failure**

- 1. You move to the greenhouse.(Score:7)
- 2. focus on flower pot 1 (Score: 5) **→replan!**
- 2. pick up flower pot 1(Score:9) --> You move the flower pot 1 to the inventory.
- 3. You move to the bedroom.(Score:7)
- 4. In bedroom, move flower pot to yellow box(Score:7) --> You move the flower pot 1 to the yellow box.
- 5. In greenhouse, pick up flower pot 6(Score:7) --> You move the flower pot 6 to the inventory.
- 6. Repeat the above 1 times.
- 7. In bedroom, move flower pot 6 to yellow box(Score:5)**→replan!**
- 7. Repeat the above 1 times.
- .....
- 18. You move to the bedroom.(Score:8)
- 19. In bedroom, move flower pot 8 to yellow box(Score:8) --> You move the flower pot 8 to the yellow box

Figure 12: The visualization of the task8

**Your task is to turn on the electric buzzer. First, focus on the electric buzzer. Then, create an electrical circuit that powers it on.**

- SwiftSage-GPT4**
- 1. look around
  - 2. teleport to workshop
  - 3. focus on electric buzzer, which is necessary to proceed with task of turning it on
  - 4. focus on electric buzzer
  - 5. connect anode of battery to terminal 1 of black wire
  - 6. connect battery anode to black wire terminal 1
  - 7. connect terminal 2 of black wire to anode of electric buzzer
  - 8. connect black wire terminal 2 to anode in electric buzzer
  - 9. connect battery cathode to red wire terminal 1
  - 10. connect terminal 2 of red wire to cathode of electric buzzer
  - 11. connect red wire terminal 2 to cathode in electric buzzer
  - 12. Wait
  - ...
- Failure, no circuit(color mismatch)**

- DGAP-GPT4**
- 1. look around
  - 2. teleport to workshop
  - 3. focus on electric buzzer to ensure all subsequent actions are directed towards activating it
  - 4. focus on electric buzzer
  - 5. connect battery anode to black wire terminal 1
  - 6. connect battery cathode to orange wire terminal 1
  - 7. connect battery cathode to terminal 1 in yellow wire
  - 8. connect black wire terminal 2 to cathode in electric buzzer
  - 9. connect orange wire terminal 2 to anode in electric buzzer
  - 10. connect terminal 2 in yellow wire to anode in buzzer
- Success**

Figure 13: The visualization of the task25